REMOVAL OF BORON FROM WATERS USING FLY ASH

A Thesis Submitted to
the Graduate School of Engineering and Science of
İzmir Institute of Technology
in Partial Fulfillment of the Requirements for the Degree of

MASTER OF SCIENCE

in Environmental Engineering
(Environmental Pollution and Control)

by
Leman SÜTÇÜ

October 2005
İZMİR

We approve the thesis of **Leman SÜTÇÜ**

Date of Signature

……
Assoc. Prof. Hürriyet POLAT — **05 October 2005**
Supervisor
Department of Chemistry
Izmir Institute of Technology

……
Assist. Prof. Talal SHAHWAN — **05 October 2005**
Co-Supervisor
Department of Chemistry
Izmir Institute of Technology

……
Assoc. Prof. Mehmet POLAT — **05 October 2005**
Co-Supervisor
Department of Chemical Engineering
Izmir Institute of Technology

……
Prof. Dr. Tamerkan ÖZGEN — **05 October 2005**
Department of Chemistry
Izmir Institute of Technology

……
Assist. Prof. Fuat DOYMAZ — **05 October 2005**
Department of Chemical Engineering
Izmir Institute of Technology

……
Assist. Prof. Aysun SOFUOĞLU — **05 October 2005**
Head of Interdisciplinary
Environmental Engineering Program
Izmir Institute of Technology

..……
Assoc. Prof. Semahat ÖZDEMİR
Head of The Graduate School

ACKNOWLEDGEMENT

I would like to express my grateful thanks to my thesis supervisor Assoc. Prof. Hürriyet Polat, co-supervisors Assoc. Prof. Mehmet Polat and Assist. Prof. Talal Shahwan and jury members Prof. Dr. Tamerkan Özgen and Assist. Prof. Fuat Doymaz for their guidance, understanding, motivations and endless support during preparation of this thesis.

I also would like to thank to Research Scientist Oya Altungöz at Chemistry Department for her valuable help in ICP measurements.

Special thanks go to all friends, research assistants and technicians in İzmir Institute of Technology for their helps and friendships.

I am also grateful to Demet Erdoğan for her help and patience during this study.

Finally, Iwould like to thank to my family for their continued patience, encouragement and financial support throughout the course of my studies.

ABSTRACT

In this study, various operational parameters were tested in order to determine the feasibility of using fly ash to remove boron from aqueous solutions. Studied parameters include time of reaction, material type, solid-liquid ratio, temperature and boron concentration. Preliminary studies revealed that the ability of Yeniköy fly ash to remove boron is similar to that achieved by amberlite under certain conditions. Therefore, Yeniköy ash was selected for sorption studies which aimed at elucidating some of the thermodynamic and kinetic profiles of the sorption process.

Experiments were performed using the batch technique at six different initial boron concentrations (10, 30, 50, 100, 250, 500 mg/L), three different temperatures (298, 308, 318 K) and time period ranging from 2 minutes up to 48 hours. The experimental results revealed that the percentage sorption of boron on Yeniköy fly ash can reach up to 100% under appropriate conditions.

Results showed that sorption of boron on Yeniköy fly ash followed pseudo-second-order kinetics. The activation energies E_a, were obtained as -90.3, -57.8 and -6.1 kJ/mole for the initial concentrations of 10, 30 and 50 mg/L, respectively.

Negative ΔH^o values were obtained for lower initial concentrations of boron (10, 30, 50 mg/L) indicating that the processes are exothermic. On the contrary, at high concentrations, positive ΔH^o values were obtained for boron sorption on fly ash indicating that the uptake process becomes endothermic. The entropy change of the sorption process was found in the range of (-234)-(158) J/mole·K. The negative ΔG^o values obtained indicated that the sorption of boron is spontaneous.

ÖZET

Bu çalışmada, sulu çözeltilerden borun uzaklaştırılması için uçucu kül kullanımının uygunluğunu belirlemek amacıyla farklı koşullar altında deneysel çalışmalar gerçekleştirilmiştir. İncelenen parametreler reaksiyon zamanını, malzeme tipini, katı-sıvı oranını, sıcaklığı ve bor konsantrasyonunu içermektedir. Boru uzaklaştırmak için kullanılan Yeniköy uçucu külü, 298 K'de 24 saat boyunca kullanılan amberlit ile yakın sonuçlar göstermiştir. Böylece, adsorpsiyon çalışmaları için Yeniköy külü seçilmiştir.

Yeniköy Termik Santralından alınan küllerdeki borat iyonlarının adsorpsiyon davranışlarının kinetik profilinin ve termodinamiklerinin etkileri araştırılmıştır. Deneyler, 6 farklı başlangıç bor konsantrasyonunda (10, 30, 50, 100, 250, 500 mg/L), 3 farklı sıcaklıkta (298, 308, 318 K) ve 2 dakikadan 48 saate kadar değişen zaman periyotlarında kesikli olarak gerçekleştirilmiştir. Deney sonuçları, uygun koşullar altında, Yeniköy külündeki borun tutunma yüzdesinin %100'lere kadar ulaşabileceğini göstermiştir.

Sonuçlar, borun Yeniköy külündeki adsorpsiyonunun pseudo-second-order kinetiğini izlediğini göstermiştir. Aktivasyon enerjileri, E_a, başlangıç konsantrasyonları olan 10, 30 ve 50 mg/L'de, -90.3, -57.8 ve -6.1 kJ/mol olarak elde edilmiştir.

Borun düşük başlangıç konsantrasyonlarında (10, 30, 50 mg/L) elde edilen negatif ΔH^o değerleri, proseslerin ekzotermik olduğunu göstermektedir. Buna paralel olarak, yüksek konsantrasyonlarda, pozitif ΔH^o değerleri, tutunma prosesinin endotermik olduğunu göstermektedir. Adsorpsiyon prosesinin entropi değişimi (-234)–(158) J/mol·K arasında bulunmuştur. Elde edilen negatif ΔG^o değerleri borun Yeniköy külü üzerine tutunma mekanizmasının kendiliğinden gerçekleştiğini göstermiştir.

Adsorpsiyon sonrası su kalitesi, ASTM prosedürlerine göre ölçüldüğünde çevresel standart değerlerinde bulunmuştur. Majör elementlerin ve ağır metallerin konsantrasyon seviyeleri kalsiyum dışında, atık sular için belirtilen standart değerlerin altındadır.

TABLE OF CONTENTS

LIST OF FIGURES

Figure **Page**

LIST OF TABLES

CHAPTER 1

INTRODUCTION

1.1. Statement of the Pollution Problem

Water stresses in the arid and semi-arid regions, like in the Mediterranean basin, result from a combination of natural climatic conditions, high human pressures, and often poor water management structures. Mediterranean water resources frequently suffer from severe salinisation problems that endanger present and future utilization as well as economic and social development of the concerned regions. Moreover, high concentrations of the element boron in the water resources make them unusable for human consumption and for irrigation purposes.

Recently boron has been classified as a pollutant of drinking water in national, EU and international drinking water directives. The recent EU drinking water directive defines an upper limit of 1 mgB/L. Moreover, boron is toxic for sensitive crops (e.g., mango, avocado, citrus fruits) at concentration levels exceeding some mg/L in irrigation water and most crops are sensitive to boron levels>0.75 mg/L in irrigation water. Entire regions in many countries that border the Mediterranean Sea suffer from boron contamination of their scarce groundwater and surface water resources, rendering them unusable for human consumption or even for irrigation purposes (Polat et al. 2004).

Some irrigation water resources, especially those in areas where geothermal waste waters are discharged, have high boron concentrations. Turkey has very rich boron and geothermal energy reserves. However, these reserves cause boron pollution by containing high boron content up to 7 mg/L. In geothermal waters, this level can be as high as 30 mg/L. For instance some of the branches of B. Menderes River in Turkey contain great amounts of Boron up to 21.1 mg/L. It has been previously shown in researches carried out by Devlet Su İşleri (State Hydraulic Works) that Boron concentrations in both some streams and some ground waters of the region have reached hazardous levels (WEB_1, 2005).

Furthermore, boron is contained in high concentrations in domestic waste water (0.5-2 mg/L) and seawater (4.7 mg/L). For years, companies added boron to detergents because it is an excellent bleaching agent – thus resulting in the formation of boron-rich sewage. Neither standard waste water treatment nor desalination of seawater by reverse osmosis is able to eliminate boron from the raw water. Residual boron contamination thus prevents these techniques from providing an alternative water supply for both drinking water and irrigation purposes.

As a precautionary measure, environmental regulators in both Cyprus and Israel have chosen a particular strategy to reduce boron contamination: mandating regulations that restrict the amount of boron that can be added to detergents. Although the reduction in boron in treated sewage may prove to be beneficial for agriculture because there will be less boron contamination in the irrigation water, these regulations will have negligible effects for improving drinking water.

For a country that will soon join the European Union, such as Cyprus, it will only be able meet its obligation to abide by E.U. standards for drinking water by pursuing an alternative strategy that calls for technological intervention to remove boron. To date, Israel has yet to adopt an official drinking water standard for boron, despite the new proposals for desalination calling for 0.5 milligrams per liter boron in desalinated water. Thus, Israel already faces a similar challenge as Cyprus.

In short, because boron contamination in all our investigated cases comes from natural geochemical background pollution and hence cannot be prevented, the only way to address the boron problem is through treatment of the drinking water.

At present in Italy and Israel, water authorities mix the boron-rich water with high-quality water to reduce the level of boron in the water supplied for both drinking and agricultural purposes. However, the longevity of dilution as a solution is limited, primarily due to the diminishing amount of high-quality water that is available. As a result, our research has focused on the creation of a new technique for boron removal from the water.

1.2. Current Methods Used to Remove Boron from Water

Boron removal has given rise to numerous works (Pilipenko et al. 1990). The main processes that have been studied are:

(1) precipitation-coagulation,

(2) adsorption on oxides (Lapp and Cooper 1976, Choi and Chen 1979, Okay et al. 1985, Pilipenko et al. 1990, Hayashi et al. 1991),

(3) adsorption on active carbon or cellulose (Choi and Chen 1979),

(4) ion exchange with basic exchangers (Peterson 1975, Popat et al. 1988),

(5) solvent extraction after complexation (Lapp and Cooper 1976, Grinstead and Wheaton 1971, Pilipenko et al. 1990, Matsumoto et al. 1997),

(6) electrodialysis (Melnik et al. 1999),

(7) reverse osmosis (Magara et al. 1996 and 1998),

(8) membrane filtration after complexation (Smith et al. 1995),

(9) use of boron selective resins, with diols as boron complexing agents, particularly Amberlite XE 243 (Lyman and Preuss 1957, Kunin and Preuss 1964, Sahin 1996) then the macroreticular resin Amberlite IRA743 (Okay et al. 1985, Recepoglu and Beker 1991) or the 564-type (Song and Huang 1987) and some other ones (Grinstead and Wheaton 1971, Ristic and Rajakovik 1996). These investigations have shown that only use of boron selective resins is adapted for drinking water, despite a high regeneration cost. It is also known that chelating resins containing functional groups in which hydroxyl groups are in the 1-2 or 1-3 position show high selectivity for boron removal through the formation of borate-diol complexes (Kunin et al. 1964, Schilde and Uhlemann 1992). Recepoğlu and Beker (1991) used Amberlite IRA 743 in the investigation of boron removal from Kızıldere geothermal wastewater; Kabay et al. (2004) employed three different chelating resins, namely Diaion CRB 01, Diaion CRB 02, and Purolite S 108 for the same purpose.

One of the most important characteristic for boron removal process is that the process must be cost efficient and easily available. Previous attempts to remove boron from water were primarily based on boron-specific ion exchange and a second cycle of reverse osmosis (RO) desalination, yet these solutions add significant cost to the overall treatment technique (Polat et al. 2004). In the case of ion exchangers, the boron removal efficiency was 90–98%, but the regeneration costs were very high. For reverse osmosis,

the removal efficiency was about 40–80% and in some cases (pH 10–11) over 90%. This technique is not effective due to membrane stability, costs, and membrane scaling because of $CaCO_3$. In electrodialysis, the removal efficiency is 40–75%; it is not appreciable and also is expensive. In co-precipitation, the removal efficiency is about 90% in the boron range of 1.6–0.16 mgB/L using $Al_2(SO_4)_3$ and $Ca(OH)_2$. This method is also not effective due to the sludge production at the end of the process. Adsorption is a cost-effective process used by other researchers. The adsorbents used were pyrohyllite (Keren et al. 1994), some acid soils (Data and Bahadoria 1999), amorphous aluminum and iron oxides, allophane, kaolinite (Su and Suarez 1995), hydrous ferric oxide (Peak et al. 2003), chitosan resin modified by saccharides (Matsumoto et al. 1999), activated carbon (Rajakovic and Ristic 1996), and clays and soils (Goldberg et al. 1996).

1.3. The Scope of the Study

The scope of this study was to investigate the removal of boron from aqueous systems (simulated wastewater) using natural coal and fly ash materials which were obtained from Soma, Yatağan and Yeniköy Power Plants. There is a growing interest in the preparation of low cost adsorbents for water treatment, so usage of natural (untreated) and abundant materials are important for the cost-cutting of the processes. Previous studies showed that boron is one of the most mobile elements in ash disposal system and a large fraction of boron in fly ash is leached with water, particularly under low pH conditions (1, 2). In contrast, this study shows that boron can also be retained by fly ash.

Batch adsorption experiments were carried out under various operational conditions such as solid/liquid ratio, reaction time, temperature, and boron concentration to study;

- Boron adsorption capacity of ash
- Adsorption kinetics and isotherms
- Residual water quality after adsorption

CHAPTER 2

BORON AND ADSORPTION ON DIFFERENT SUBSTRATES

2.1. Discussion on Boron

2.1.1. Environmental Occurrences and Concentrations

The element boron (B) is widely distributed in nature. Because of its high affinity for oxygen, boron always occurs in nature bound to oxygen in the form of inorganic borates. Apart from their occurrence in a few commercially exploitable deposits (mainly as sodium or calcium borate minerals), the borates are present everywhere at low concentrations in rocks (15–300 mgB/kg), soils (<10–20 mgB/kg), fresh waters (<1 mgB/L) and sea water (5 mgB/L). The content of boron in the lithosphere by mass is about 1.10^{-3} %. Table 2.1 gives data on the distribution of boron in various components of the earth's crust.

The world's oceans have by far the greatest content of borate, with an average concentration of 5 mgB/L. Lakes and rivers in most parts of the world, except in areas of volcanic activity with more elevated concentrations, contain an environmental background content of <1 mgB/L, generally between 0.01 to 0.3 mgB/L. No typical concentration of borate can be cited for groundwater, which includes flowing springs (both hot and cold), geysers, aquifers (both flowing and confined), oilfield brines, etc. The recent review of the borate content of European ground waters shows that values can vary from <0.1 to >1 mgB/L and are dependent upon geological circumstances, especially in areas of volcanic activity. Mineral waters contain a range of from < 0.02–4.3 mgB/L (ECETOC 1997).

Table 2.1. Distribution of boron
(Source: Walker 1975)

Source	***Weight %***	***Source***	***Weight %***
Earth's Crust	$1*10^{-3}$	Meteorites	$3*10^{-4}$
Inside rocks	$1*10^{-4}$	Sea water (dry residue)	$1.5*10^{-2}$
Acid rocks (granites, etc.)	$1.5*10^{-3}$	Salt springs (dry residue)	$(3\text{-}20)*10^{-3}$
Sedimentary rocks	$1.2*10^{-2}$	Salt lakes (dry residue)	$(1\text{-}60)*10^{-2}$
Soils	$1*10^{-3}$	Water of mud volcanoes (dry residue)	$(6\text{-}400)*10^{-2}$
Granite pegmatites	$(1\text{-}10)*10^{-2}$	Petroleum brine	$(1\text{-}60)*10^{-2}$
Marine clays	$5*10^{-2}$	Marine plants (ash)	$1.5*10^{-1}$
Iron ores (maritime)	$5*10^{-2}$	Marine animals (ash)	$(3\text{-}100)*10^{-4}$
Iron ores (nonmaritime)	$5*10^{-4}$	Rye, wheat, oats and other grains (dry matter)	$(0.6\text{-}36)*10^{-4}$
Lime stones	$5*10^{-4}$	Clover, alfalfa (dry matter)	$(7\text{-}57)*10^{-4}$

Igneous rocks generally have low borate content. Sedimentary rocks have a higher borate content, which is related to the salinity of the water at the time of deposition. The borate content from such marine segments ranges from 15–300 mgB/kg. The weathering of rocks, by rainfall and by erosion from rivers, provides a continuous small source of borate into the soil and the aqueous environment. Soils of low borate content (<10mgB/kg) are present on most of the earth. The average of overall content of borate of all soils is 10–20 mgB/kg, with higher values (up to 100 mgB/kg) in the western USA and across the Mediterranean in Turkey, Iran, Kazakhstan (ECETOC 1997).

Although few data are available, the level of borate in the atmosphere is low and around 16 ngB/m^3 according to a recent estimate. Its presence probably arises mainly from the vapor pressure of boric acid above the seawater. The tropospheric burdens for particulate and gas-phase boron were recently estimated to be 6,000 tons and 60,000 to 110,000 tons, respectively (ECETOC 1997).

Large deposits of borate minerals are rare. The only known massive deposits are located in the Mojave Desert of California, USA, and in western Turkey. The four most important minerals are colemanite, kernite, tincal and ulexite.

The world boron reserve is 885 billion tons and Turkey has 64% of these boron reserves. The distribution of boron reserves in the world and in Turkey is given in Table 2.2 and Table 2.3, respectively.

Table 2.2. Boron reserves in the world (million tons, as B_2O_3)
(Source: Kılıç 2004)

	Proven Economic Reserve	***Probable & Possible Reserve***	***Total Reserve***	***% in Total Reserve***	***Reserve Life-span (year)***
Turkey	224,000	339,000	563,000	64	389
USA	40,000	40,000	80,000	9	55
Russia	40,000	60,000	100,000	11	69
China	27,000	9,000	36,000	4	25
Chile	8,000	33,000	41,000	5	28
Bolivia	4,000	15,000	19,000	2	13
Peru	4,000	18,000	22,000	2	15
Argentina	2,000	7,000	9,000	1	6
Kazakhstan	14,000	1,000	15,000	2	10
TOTAL	***363,000***	***522,000***	***885,000***	***100***	***610***

Table 2.3. Boron reserves in Turkey

(Source: Kılıç 2004)

Production Area	*Mineral*	*Reserve Million Tons*	*Content of B_2O_3 %*	*Capacity (Ton / Year)*	*Production (Ton / Year)*
Kırka Bor İşletmesi	Tincal	605.5	25.8	200,000	558
Bigadiç Bor İşletmesi	Ulexite	49.2	29.1	200,000	200
	Colemanite	576.4	29.4	200,000	90
Emet Bor İşletmesi	Colemanite	835.6	27.5-28.5	500,000	300
Kestelek Bor İşletmesi	Colemanite	7.7	25-33.2	100,000	60
TOTAL		***2074.4***		***1,200,000***	***1208***

2.1.2. Physical and Chemical Properties

Boron is the first element of group III A, with atomic number of 5. The boron atom contains five electrons, two in the inner shell (the K electrons) and three in the outer shell (the L electrons). The ground state electron configuration of boron is $1s^2 2s^2 2p^1$.

Two stable isotopes of boron, B^{10} and B^{11}, are known in nature. Naturel mixtures contain 18.83% B^{10} and 81.17% B^{11} (Budavari et al. 1989).

Elementary boron exists in two forms such as fine crystalline and crystalline. Fine-crystalline so-called amorphous boron is brown in color while crystalline boron is dark grey. Boron is a relatively inert metalloid except when in contact with strong oxidizing agents.

Sodium perborates are persalts, which are hydrolytically unstable because they contain characteristic boron–oxygen–oxygen bonds that react with water to form hydrogen peroxide and stable sodium metaborate ($NaBO_2 \cdot nH_2O$).

The relative abundance of the two aqueous species of boron (borate; $B(OH)_4^-$ and boric acid; $B(OH)_3$), is pH dependent. Boric acid is a weak acid, with a pK_a of 9.15, and therefore boric acid and the sodium borates exist predominantly as undissociated boric acid [$B(OH)_3$] in dilute aqueous solution at pH<7; at pH>10, the metaborate anion $B(OH)_4^-$ becomes the main species in solution.

$$B(OH)_3 + NaOH \longleftrightarrow [B(OH)_4]^- + Na^+$$

Between these two pH values, from about 6 to 11, and at high concentration (>0.025 mole/liter), highly water soluble polyborate ions such as $B_3O_3(OH)_4^-$, $B_4O_5(OH)_4^-$, and $B_5O_6(OH)_4^-$ are formed.

$$2\ B(OH)_3 + [B(OH)_4]^- \longleftrightarrow [B_3O_3(OH)_4]^- + 3\ H_2O$$

Due to a large isotopic fractionation (approximately 20 ‰) that occurs between the two chemical species in natural seawater, it can be shown that their respective boron isotopic compositions are also pH dependent (Figure 2.1.).

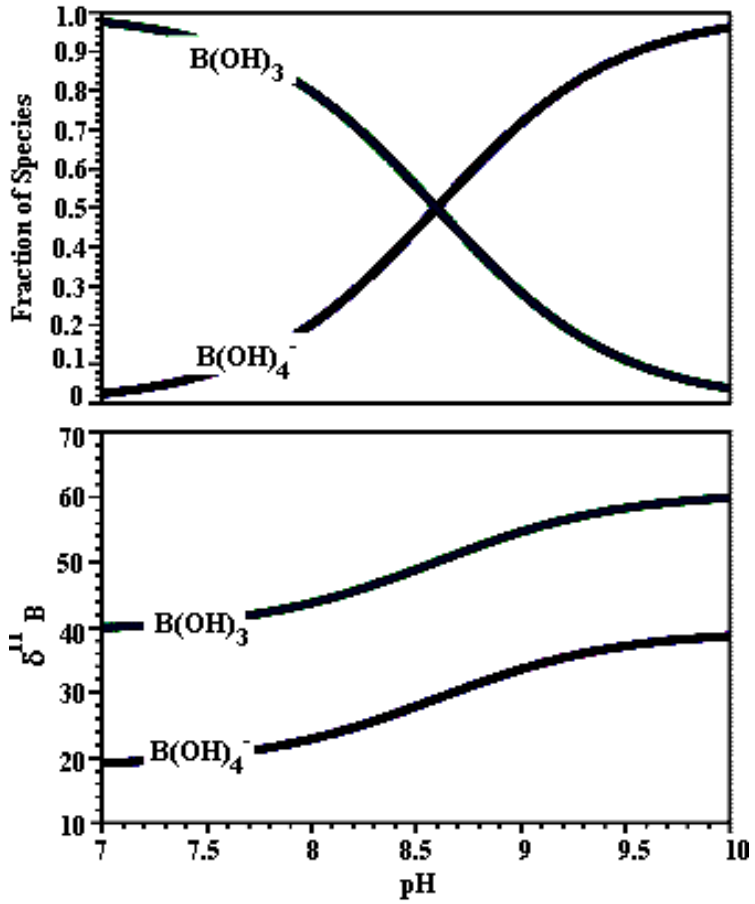

Figure 2.1. pH dependent boron composition

The chemical and toxicological properties of borax pentahydrate $Na_2B_4O_7 \cdot 5H_2O$, borax $Na_2B_4O_7 \cdot 10H_2O$, boric acid, and other borates are expected to be similar on a molar boron equivalent basis when dissolved in water or biological fluids at the same pH and low concentration (WHO 1998). The basic physicochemical properties of boron are shown in Table 2.4 (ACM 1997).

Table 2.4. Physical properties of boron

Property	***Value***
Atomic weight	10.81 ± 0.005
Melting point	2190 ± 20 ºC
Boiling point	3660 ºC
Density of boron (Crystalline, 25 – 27 ºC)	2.33 ± 0.02 g/cm^3
Density of boron (Amorphous, 25 - 27 ºC)	2.3 g/cm^3
Hardness, mineralogical scale	9.3
Heat capacity (25 - 927 ºC)	1.54 + 0.0044 · T cal/g-atom · deg
Heat of combustion	306 ± 1 kcal/g-atom
Heat of transition, $B_{am} \rightarrow B_{cryst}$	0.4 kcal/g-atom
Heat of vaporization	128 kcal/g-atom
Heat of fusion	5.3 kcal/g-atom
Mohs hardness	11
Knoop hardness	2100 - 2580 HK
Vickers hardness	5000 HV
Oxidation number	3
Electronegativity	2
Atomic radius	1.78 Å
Ionic radius of B^{3+}	0.23 Å

Boron has the highest electropositivity value after diamond among ametals. Its electric conductivity is low at room temperature and high at high temperatures.

2.1.3. Usage Areas

Boron forms several commercially important compounds. The most important boron compound is sodium borate pentahydrate ($Na_2B_4O_7 \cdot 5H_2O$). Large amounts of this compound are used in the manufacture of fiberglass insulation and sodium perborate bleach. The second most important compound is boric acid (H_3BO_3), which is used to manufacture textile fiberglass and is used in cellulose insulation as a flame retardant. Sodium borate decahydrate ($Na_2B_4O_7 \cdot 10H_2O$), better known as borax, is the third most important boron compound. Borax is used in laundry products and as a mild antiseptic.

Boron compounds are widely employed in many branches of the national economy, for example in medicine for the preparation of disinfectants and drugs, in the glass industry for the production of optic and chemically stable glass (glass products use 53.6% of the boron consumption in the United States, and 32.7% in Western Europe (Butterwick et al. 1989)), as components of enamels to increase hardness, for the protection of metals against oxidation during soldering, as additives to electrolytes in nickel plating, in the production of heat resistant polymers and also as catalysts. Boron compounds are also used in cosmetic, leather, textile, rubber and paint industries. They also find application in the wood-processing industry as a protection against molds (ECETOC 1995).

Boron is used in pyrotechnics and flares to produce a green color. Boron has also been used in some rockets as an ignition source. Boron-10, one of the naturally occurring isotopes of boron, is a good absorber of neutrons and is used in the control rods of nuclear reactors, as a radiation shield and as a neutron detector. Boron filaments are used in the aerospace industry because of their high-strength and lightweight.

Cleaning and washing products also use boron compounds. In North America, boron is mostly used as a washing aid and softener where ten percent of boron consumption is used in the cleaning industry. In Western Europe, sodium perborate is used as a bleaching agent in soap and detergent. Over 41% of their boron consumption is in cleaning products (Butterwick et al. 1989).

Boron, an essential trace element for plant growth, is often added to crops in a fertilizer. In higher concentrations, it can also be used as a non-selective herbicide for weed control, insecticide, algaecide in water treatment and as a timber preservative. The

United States uses approximately 5% of its boron consumption in the agrochemical field (Butterwick et al. 1989).

2.1.4. Toxicity

Although boron is an essential nutrient for higher plants, it is not currently considered essential for mammals as it has not been possible to establish that deficiency impairs biological function. However, it is thought that low dietary levels protect against fluorosis and bone demineralization and may indirectly influence calcium, phosphorus, magnesium and cholecalciferol (vitamin D3) metabolism (Health Canada 1990, Eisler 1990). In high doses (about 100 mg), though, boron can be toxic. Toxic effects include a red rash with weeping skin, vomiting, diarrhea characterized by a blue green color, depressed blood circulation, coma and convulsions. A fatal dose in adults is 15 to 20 g and in children 3 to 6 g repeated intakes of small amounts can cause accumulative toxicity.

The current interim maximum acceptable concentration for boron in drinking water, from Health Canada, is 5.0 mg/L (Health Canada 1996). The National Academy of Sciences (1980) recommends a guideline of less than 1.0 mgB/L for drinking water. In the Russia, the guideline is less than 0.5 mgB/L (Seal and Weeth 1980), and according to Puls (1994), the recommended maximum levels for humans is less than 5.0 mgB/L. According to the US Environmental Protection Agency (WEB_2, 2003), Office of Water (1996), the reference dose of boron for a 70 kg adult is 0.9 mg/kg day. This is an estimate of a daily exposure to the human population that is likely to be without appreciable risk of deleterious effect over a lifetime.

It is generally accepted that boron toxicity is closely associated with salinity problems in hot, arid climates (Butterwick et al. 1989, Nicholaichuk et al. 1988, Gupta et al. 1985). However, toxic levels do not occur on agricultural lands unless boron compounds have been added in excessive quantities, such as with fertilizer materials, irrigation water sewage sludge or coal ash (Eisler 1990). Irrigation water contaminated with boron is one of the main causes of boron toxicity in plants and it is the continued use and concentration of boron in soil, especially in arid regions with high evapotranspiration that leads to toxicity problems (Gupta et al. 1985). Boron toxicity in plants is characterized by stunted growth, leaf malformation, browning and yellowing,

chlorosis, necrosis, increased sensitivity to mildew, wilting and inhibition of pollen germination and pollen tube growth (Butterwick et al. 1989, Eisler 1990).

The limits between boron deficiency and toxicity are very narrow, so boron applications can be extremely toxic to some plants at concentrations that are only slightly above optimum for others (Gupta et al. 1985). Boron deficiency or excess will result in the reduction of crop yield and/or the impairment of crop quality. Generally, boron toxicity under field conditions occurs when plant tissue concentrations exceed 0.2 mg/g (dry weight). Sensitive crops may experience toxicity below this level (Gupta et al. 1985).

It is recommended that the maximum concentration of boron for the protection of irrigated crops should not exceed those shown in Table 2.5. These guidelines depend on the sensitivity of the crops and are consistent with the Canadian Council of Ministers of the Environment (CCME 1999) guidelines.

Table 2.5. Relative tolerance of agricultural crops to boron
(Source: CCME 1999)

Tolerance	***Concentration of B in irrigation water (mg/L)***	***Agricultural Crop***
Very sensitive	<0.5	blackberry
Sensitive	0.5-1.0	peach, cherry, plum, grape, cowpea, onion, garlic, sweet, potato, wheat, barley, sunflower, mung bean, sesame, lupin, strawberry, Jerusalem artichoke, kidney bean, lima bean
Moderately sensitive	1.0-2.0	red pepper, pea, carrot, radish, potato, cucumber
Moderately tolerant	2.0-4.0	lettuce, cabbage, celery, turnip, Kentucky bluegrass, oat, corn, artichoke, tobacco, mustard, clover, squash, muskmelon
Tolerant	4.0-6.0	sorghum, tomato, alfalfa, purple vetch, parsley, red beet, sugar beet
Very tolerant	6.0-15.0	asparagus

Table 2.6. Recommended guidelines
(Source: CCME 1999)

Drinking water	5.0 mgB/L
Fresh water aquatic life	1.2 mgB/L
Marine aquatic life	1.2 mgB/L
Wildlife	5.0 mgB/L
Irrigation	Depends upon crop (see Table 2.5)
Livestock watering	5.0 mgB/L

2.2. Adsorption Process and Boron Adsorption on Different Substances

2.2.1. Adsorption Process

Adsorption is the process of accumulating substances that are in solution on a suitable interface. Adsorption is a mass transfer operation in that a constituent in the liquid phase is transferred to the solid phase. The *adsorbate* is the substance that is being removed from the liquid phase at the interface. The *adsorbent* is the solid, liquid or gas phase onto which the adsorbate accumulates. Although adsorption is used at the air-liquid interface, only the case of adsorption at the liquid-solid interface will be discussed in this study.

The term adsorption is used also to describe two kinds of forces of interaction between the adsorbate and the adsorbent. These interaction forces are broadly described as *physisorption* (physical adsorption) and *chemisorption* (chemical adsorption). The basic characteristics of them are given below in Table 2.7 (Rouquerol 1999).

Physical adsorption (physisorption) is relatively non-specific and is due to the operation of weak forces between molecules. In this process, the adsorbed molecule is not affixed to a particular site on the solid surface; it is free to move over the surface

(Sawyer et. al. 1994). The physical interactions among molecules, based on electrostatic forces, include dipole-dipole interactions, dispersion interactions and hydrogen bonding. When there is a net separation of positive and negative charges within a molecule, it is said to have a dipole moment. Molecules such as H_2O and N_2 have permanent dipoles because of the configuration of atoms and electrons within them. Hydrogen bonding is a special case of dipole-dipole interaction and hydrogen atom in a molecule has a partial positive charge. Positively charged hydrogen atom attracts an atom on another molecule which has a partial negative charge. When two neutral molecules which have no permanent dipoles approach each other, a weak polarization is induced because of interactions between the molecules, known as the dispersion interaction (Montgomery 1985). Figure 2.2 illustrates the main interactions and forces during physical adsorption processes.

Table 2.7. Properties of physisorption and chemisorption

Physisorption	**Chemisorption**
✓ Multilayer adsorption	✓ Monolayer adsorption
✓ Low degree of specificity	✓ Depends on the reactivity of adsorbent and adsorbable substance
✓ Desorption is possible (sorbed molecule keeps its identity)	✓ Desorption is impossible (sorbed molecule loses its identity)
✓ Always exothermic (energy involved is <~40kJ/mole)	✓ Exothermic or endothermic, chemical bond forms (energy involved can reach several hundreds of kJ/mole)
✓ System generally reaches thermodynamic equilibrium rapidly	✓ Activation energy is involved and at low temperatures, system may not reach equilibrium

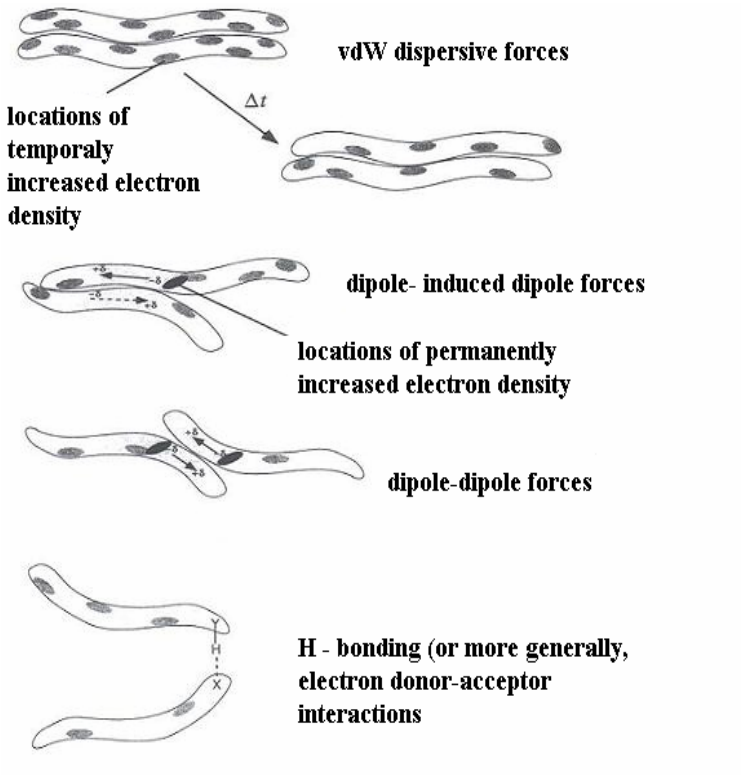

Figure 2.2. Illustration of the various molecular interactions arising from uneven electron distributions (Source: Schwarzenbach 2003).

Chemical adsorption, (chemisorption) is also based on electrostatic forces, but much stronger forces act a major role on this process (Sawyer et al. 1994). In chemisorption, the attraction between adsorbent and adsorbate is a covalent or electrostatic chemical bond between atoms, with shorter bond length and higher bond energy (Montgomery 1985).

The enthalpy of chemisorption is very much greater than that for physisorption, and typical values are in the region of 200 kJ/mole, whereas this value for physisorption is about 20 kJ/mole. Except in special cases, chemisorption is exothermic. A spontaneous process requires a negative free energy (ΔG) value. Because, the translational freedom of the adsorbate is reduced when it is adsorbed, entropy (ΔS) is usually negative. Therefore, in order for $\Delta G = \Delta H - T\Delta S$ to be negative, ΔH is expected to be negative, and the process is exothermic. If the enthalpy values less negative than -25 kJ/mole, system is physisorption and if the values more negative than -40 kJ/mole it is signified as chemisorption (Atkins 1994).

Table 2.8. The bond energies of various mechanisms for adsorption
(Source: Atkins 1994)

Interaction between adsorbent and adsorbate	**Enthalpy (kJ/mole)**		
	-ΔH	**+ΔH**	
Electrostatic chemical bonding	> 40	> 200	chemisorption
Dispersion interactions and hydrogen bonding	8 - 40		physisorption
Dipole-dipole interaction	< 8	< 20	physisorption

2.2.2. The Liquid – Solid Interface

The interaction of ions in the hydrosphere with soil components is subject to various types of factors. These factors are related with the properties of groundwater (temperature, pH, E_h), the speciation of these cations and their concentrations, the structural characteristics of the soil components like porosity, surface area, swelling, grain size, in addition to them, factors that include period of contact, degree of mixing and solid/liquid ratio.

The adsorption process, as illustrated on Figure 2.3, takes place in four more or less definable steps: (1) bulk solution transport, (2) film diffusion transport, (3) pore transport and, (4) adsorption. *Bulk solution transport* involves the movement of the material to be adsorbed through the bulk liquid to the boundary layer of fixed film of liquid surrounding the adsorbent, typically by advection and dispersion. *Film diffusion transport,* involves the transport by diffusion of the material through the stagnant liquid film to the entrance of the pores of the adsorbent. *Pore transport* involves the transport of the material to be adsorbed through the pores by a combination of molecular diffusion through the pore liquid and/or by diffusion along the surface of the adsorbent. *Adsorption* involves the attachment of adsorbate to adsorbent at an available adsorption site (Metcalf and Eddy 2003).

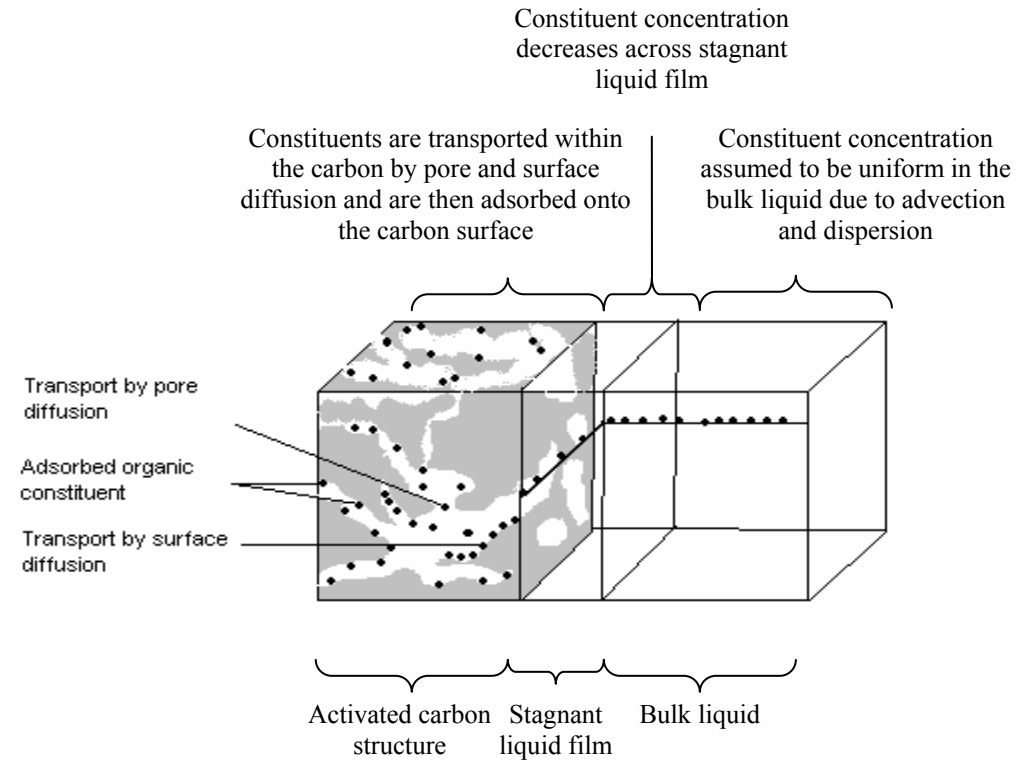

Figure 2.3. Schematic for adsorption of an organic constituent with activated carbon (Source: Metcalf and Eddy 2003)

Adsorption can occur on the outer surface of the adsorbent and in the macropores, mesopores, micropores, and submicropores, but the surface area of the macro and mesopores is small compared with the surface area of the micropores and submicropores and the amount of material adsorbed there is usually considered negligible.

The type of diffusion in an ion exchange process is affected by soil particle size and nuclide concentration. Film diffusion occurs usually with a low concentration and small-sized particles. Soil mineral composition affects the amount of exchanging cations. Also many factors such as ion exchange, soil particle radius, and organic constituents affect the rate of ion exchange on soils. Usually the rate of ion exchange declines with increasing charge of the exchanging species (Liu et al. 1995).

2.2.3. Adsorption Isotherms

The relation between amount adsorbed and concentration is known as the adsorption isotherm. Adsorption equilibrium data are typically plotted in the form of an adsorption isotherm with the mass adsorbed on the y-axis and the mass in the fluid on the x-axis at constant temperature.

Sorption isotherms are mathematical models that describe the distribution of the sorbate specie among liquid and solid phases, based on a set of assumptions that are related to the heterogeneity/homogeneity of the solid surface, the type of coverage, and the possibility of interaction between the sorbate specie.

Freundlich Isotherm: A brief empirical equation often used to represent adsorption data is called the Freundlich equation. The Freundlich isotherm describes physical adsorption from liquids (Brev 1958).

The empirically derived Freundlich isotherm is defined as follows.

$$q_e = K_f \cdot C_e^{1/n} \tag{2.1}$$

where; q_e : amount adsorbate adsorbed per unit weight of adsorbent at equilibrium

C_e : equilibrium concentration of adsorbate in solution after adsorption

K_f : empirical Freundlich constant or capacity factor (mg/g), (mol/L)

$1/n$: the Freundlich exponent.

The exponent $1/n$ is an index of the diversity of free energies associated with the sorption of the solute by multiple components of a heterogeneous sorbent. When $1/n$=1, the isotherm is linear and system has a constant free energy at all sorbate concentrations. When $1/n < 1$, the isotherm is concave and sorbates are bound with weaker and weaker free energies, finally, when $1/n > 1$, the isotherm is convex and more sorbate presence in the sorbent enhance the free energies of further sorption (Schwarzenbach 2003).

The good fit of Freundlich isotherm to an adsorption system means there is almost no limit to the amount adsorbed and there is a multilayer adsorption. The

applicability of the Freundlich equation to a particular case is tested by plotting $log\ q_e$ against $log\ C_e$ from the logarithmic form of Equation 2.1.

$$log\ q_e = log\ K_f + 1/n\ log\ C_e \qquad (2.2)$$

such a plot should yield a straight line with intercept equal to $log\ K_f$ and slope equal to $1/n$.

Langmuir Isotherm: An alternative equation was derived by Langmuir on the basis of a definite case of the nature of the process of adsorption from solution. The Langmuir adsorption isotherm was developed assuming that;

1. A fixed number of accessible sites are available on the adsorbent surface, all of which have the same energy.
2. Adsorption is reversible.
3. Monolayer adsorption occurs.
4. There are no lateral interactions among the adsorbates.

The Langmuir adsorption isotherm is defined as

$$q_e = (q_0 K_L C_e) / (1 + K_L C_e) \qquad (2.3)$$

where; q_e : amount adsorbate adsorbed per unit weight of adsorbent at equilibrium

C_e : equilibrium concentration of adsorbate in solution after adsorption

q_0 : empirical Langmuir constant which represents maximum adsorption capacity (mg/g)

K_L : empirical Langmuir constant (L/mg) (Finqueneisel 1998)

The q_0 represents the total number of surface sites per mass of adsorbent. In the ideal case, q_0 would be equal for all sorbates. However, q_0 may vary somewhat between different compounds because of differences in sorbate sizes. Therefore, it usually represents the maximum achievable surface concentration of a given compound. The constant K_L which is commonly referred to as the Langmuir constant is defined as the equilibrium constant of the sorption reaction. The K_L also implies a constant sorbate affinity for all surface sites (Schwarzenbach 2003).

Assuming the above equation (Eq. 2.3) as (Eq. 2.4),

$$C_e / q_e = (1/q_o K_L) + (1/q_o) C_e \quad (2.4)$$

and plotting of C_e / q_e vs C_e give a straight line with slope $1/q_o$ and intercept $1/q_o K_L$.

The Langmuir isotherm is limited in its application to adsorption in monolayer. It applies well to chemical adsorption and to physical adsorption when saturation is approached (Brev 1958).

Dubinin-Radushkevich (D-R) Isotherm: This model is good at low concentration ranges and can be used to describe sorption on both homogeneous and heterogeneous surfaces (Shahwan and Erten 2002).

The D-R isotherm is defined as follows (Yurdakoç et al. 2004),

$$q_e = q_m \exp(-K\varepsilon^2) \quad (2.5)$$

where q_e : amount adsorbed per unit weight of solid (mole/g)

q_m : sorption capacity of adsorbent per unit weight (mole/g)

K : constant related to the energy of sorption (mol^2/kJ^2)

ε : Polanyi potential = $RTln(1 + 1/(C_e))$ (kJ/mole)

C_e : equilibrium concentration of solute in solution (mole/g)

R : gas constant (kJ/mole K)

T = absolute temperature (K)

The linear form of the equation may be obtained by rearranging it:

$$\ln q_e = \ln q_m - K\varepsilon^2 \quad (2.6)$$

By plotting $\ln q_e$ versus ε^2, K and $\ln q_m$ can be calculated from the slope and intercept, respectively.

D-R model is used to obtain the maximum adsorption capacity q_m and mean adsorption energy E whose magnitude is useful for estimating the mechanism of adsorption. Polanyi defines the adsorption potential ε as the free-energy change required

to transfer one mole of ion from infinity in solution to the solid surface and it changes with the concentration of solution. Energy range of mean energy of sorption is within 8-16 kJ/mole for ion-exchange reactions.

The parameter *K* is related to the adsorption mean free energy as;

$$E = (-2K)^{-1/2} \quad (2.7)$$

Since D-R model does not require an energetically homogeneous surface or a constant adsorption potential, it is more common than Langmuir model. Because real surfaces are not homogeneous and binding sites are not uniform because of structural irregularities on surface (Akar 2005).

2.2.4. Boron Adsorption on Different Substrate Surfaces

It was reported that the adsorption method was economically promising for the removal of a minor constituent from a multi component solution. There had been many studies on the development of adsorbents for boron and its adsorptive properties. Boron selective adsorbents were classified into two groups as inorganic and organic. Activated carbon, activated alumina, hydrous cerium oxide and hydrous lanthanum oxide showed a high selectivity for boron among inorganic adsorbents. The organic adsorbents with polyol groups in arrangement had a selective adsorptivity for boron. N-glucamine type resin was the most promising among the natural and synthetic organic adsorbents.

Ooi et al. described the screening results of various adsorbents for boron in brine, some hydrous oxides of tetravalent metal ($HfO_2 \cdot nH_2O$, $CeO_2 \cdot nH_2O$, $ZrO_2 \cdot nH_2O$) or pentavalent metal ($Ta_2O_5 \cdot nH_2O$) showed good adsorptivity for boron. Hydrous oxides of trivalent metal didn't show a high boron adsorptivity (except for the double oxide of aluminum and iron) although they were known as anion exchangeable hydrous aluminum oxides and hydrous iron oxides had a high adsorptivity for SO_4^{-2} ions (Ooi, K., Sonoda, A. & Hirotsu, T., 1996). Since the brine contained a considerable number of sulfate ions, the competing adsorption of SO_4^{-2} on the particle surface depressed the boron adsorption. Hydrous oxides of tetravalent metal, the order of boron uptake correlated comparatively well with decreasing order of acidity of the oxides ($MnO_2 < SiO_2 < SNO_2 < TiO_2 < ZrO_2 < CeO_2$). $CeO_2 \cdot nH_2O$ gave the highest boron uptake among the hydrous metal oxides studied, in spite of the fact that it had a

relatively large crystallite size (corresponding to a small number of surface OH groups). The surface OH groups on $CeO_2 \cdot nH_2O$ had a suitable geometry and/or suitable chemical properties to fix $B(OH)_3$ by the chelation mechanism.

The boron uptakes by metal phosphates, metal oxalates, metal sulfides and other inorganic materials were also studied by Ooi et al. The boron uptakes were less than 2 mg/g for the samples sceened (Ooi et al. 1996).

H.Polat et al. (2003) presented an alternative methodology for boron removal by using several types of coal and fly ash as adsorbents. They examined the effect of pH, solid/liquid ratio, time of reaction, pre-treatment, regeneration on the boron removal capacity and the overall chemical composition of the residual. They conducted various column and batch experiments that explored the efficiency of boron removal from sea water and desalinated sea water. The results showed that the selected coal and fly ash materials were very effective such that the rejection ratio of boron could reach 95% of the initial boron content under certain optimal conditions (pH=9, solid/liquid =1/10, reaction time > 6h). Use of glycerin enabled regeneration of boron uptake into coal, but the boron uptake capacity of fly ash reduced after several cycles of treatment. They proposed that the reaction of Ca-rich fly ash with Mg-rich seawater caused co-precipitation of magnesium hydroxide in which boron was co-precipitated.

Keren et al. (1994) elucidated the dynamic aspects of the adsorption–desorption of borate ions on edge surfaces of 2:1 clay minerals. Data and Bahadoria (1999) determined the influence of soil properties on adsorption on boron. Su and Suarez (1995) studied boron adsorption on amorphous aluminum and iron hydroxides and kaolinite as a function of pH and initial B concentration. Peak et al. (2003) investigated the mechanism of boric acid and borate adsorption on hydrous ferric oxide by using ATR-FTIR. Matsumoto et al. (1999) tried to develop an environmentally friendly resin for boron removal from a boron mine and the desulfurizing equipment in coal-fired steam power stations. Rajakovic and Ristic (1996) used activated carbon impregnated with various compounds to separate the boric acid and borax from aqueous solution. Goldberg et al. (1996) examined boron adsorption on the clay minerals kaolinite and montmorillonite and two arid zone soils as a function of pH and the presence of competing anions such as nitrate and sulfate. Adsorption is a very promising technique which is very fast in the initial 2–3 contact hours; 80–99% of the total removal took in the initial 30 min, and equilibrium was attained within 2 h, when $Mg(OH)_2$ was used as

adsorbent. On the other hand, kinetic and thermodynamic parameters of these adsorption processes have not been examined yet.

2.3. Fly Ash as an Alternative Adsorbent Material

Fly ash is the by-product of the coal combustion process for energy generation, and is recognized as an environmental pollutant. Because of environmental problem of fly ash as a good deal of work and applications on the utilization of fly ash has been undertaken in the world.

One of the utilization areas of fly ash as the adsorption of metallic ions at liquid/solid interface has been studied for several years, as well as the use of some so-called low cost sorbents. Moreover, fly ashes produced by coal combustion are considered in numerous studies aimed at their valorization. Different applications (cements, roads and backfill) already allow a recycling of an important part of fly ash production which, for instance, reached 450,000 tons in 1997 in France. The use of fly ashes for metallic ions removal from aqueous solution is today's interest and some experiments have showed that fly ashes might be beneficial for removal of heavy metal ions in waste waters (Rio and Delebarre 2003).

2.3.1. Definition of Fly Ash

The fly ash produced from the burning of pulverized coal in a coal-fired boiler is a fine-grained, powdery particulate material that is carried off in the flue gas and usually collected from the flue gas by means of electrostatic precipitators, baghouses, or mechanical collection devices such as cyclones. The term fly ash is not applied to the residue extracted from the bottom of boilers. A general flow diagram of fly ash production in a dry-bottom coal-fired utility boiler operation is presented in Figure 2.3.

Fly ash is defined as "the finely divided residue resulting from the combustion of ground or powdered coal which is transported from the firebox through the boiler by flue gases; known in UK as pulverized fuelash (pfa)" (ACI Committee (226) 1987, Dermatas and Meng 2003).

Fly ashes may be sub-divided into two categories, according to their origin (ASTM):

Class F : Fly ash normally produced by burning anthracite or bituminous coal which meets the requirements applicable to this class.

Class C : Fly ash normally produced by burning lignite or sub-bituminous coal which meets the requirements applicable to this class. Class C fly ash possesses some cementitious properties. Some Class C fly ashes may have lime contents in excess of 10 % (Weshe 1991).

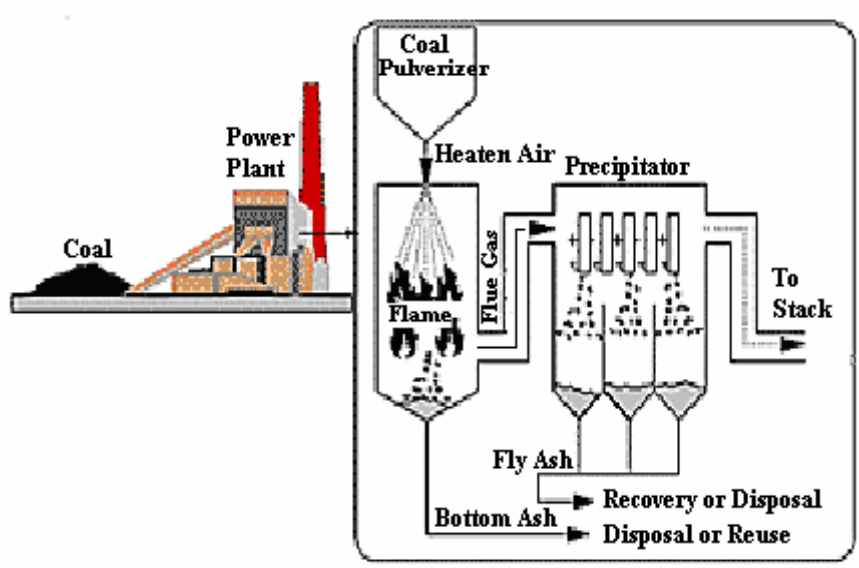

Figure 2.4. Production of fly ash in a dry-bottom utility boiler with electrostatic precipitator.

Bottom ash is the ash which is removed from a fixed grate by hand or which falls by gravity from the combustion zone. It is coarser and heavier than fly ash particles. Bottom ash forms when ash particles agglomerate to form aggregates similar to volcanic rock.

Slag is the material retained in the furnace. It is a kind of a solidified molten ash. Hence, the material is glassy and the larger pieces resemble obsidian. Compared to bottom ash, slag may have slightly higher bulk density and lower absorption capacity (Çancı 1998).

2.3.2. Composition of Fly Ash

Mineralogical Composition: The chemical and mineralogical composition of fly ashes depends upon the characteristics and composition of the coal burned in the power plant. Owing to the rapid cooling of the material, fly ashes are composed mainly (50-90 %) of mineral matter in the form of glassy particles. A small amount of ash occurs in the form of crystals. Unburned coal is collected with the fly ash as particles of carbon, which may constitute up to 16 % of the total, depending on the rate and temperature of combustion, the degree of pulverization of the original coal, the fuel/air ratio, the nature of the coal being burned, etc.

The most important minerals found in fly ashes from bituminous coal are:

Magnetite	0.8 - 6.5%
Hematite	1.1 - 2.7%
Quartz	2.2 - 8.5%
Mullite	6.5 - 9.0%
Free calcium oxide	up to 3.5%

Other minerals like goethite, pyrite, calcite, anhydrite and periclase range from trace amounts to 2.5 % (Weshe 1991).

Geochemistry of Fly Ash: The elements in the fly ash are mainly litophiles and chalcophiles. Lithophiles are the elements that are concentrated in aluminosilicates as oxide forms rather than in the metallic and sulfide phases. They are mainly, Al, Ca, K, Mg, Na, Si and the rare earth elements. Chalcophiles are the elements that are concentrated in the sulfide phases rather than in the metallic and silicate phases. They are mainly, As, Cd, Ga, Ge, Pb, Sb, Sn, Tl and Zn. Being nonvolatile, lithophiles form the matrix of fly ashes. Chalcophiles, on the other hand, are volatile elements and are associated with the non-matrix structure. They are concentrated at the surface of the fly ashes. Br, Cl and F are halogens which remain mainly in the gas phase. Others, such as Ba, Be, Bi, Co, Cr, Cu, Mn, Ni, U, V and W are intermediate, showing an equal distribution between the matrix and non-matrix structure.

The matrix of fly ash particles is principally composed of aluminum-silicon-oxygen compounds (non-volatile oxides of the major elements), with smaller amounts of Fe, Mg, Na, K, Ca, Th, Ti and the rare earth elements. This structure is commonly called the aluminosilicate matrix (Çancı 1998).

2.3.3. Material Properties

2.3.3.1. Physical Properties

Fly ash consists of fine, powdery particles that are predominantly spherical in shape, either solid or hollow, and mostly glassy (amorphous) in nature. The carbonaceous material in fly ash is composed of angular particles. The particle size distribution of most bituminous coal fly ashes is generally similar to that of a silt (less than a 0.075 mm or No. 200 sieve). Although subbituminous coal fly ashes are also silt-sized, they are generally slightly coarser than bituminous coal fly ashes (DiGioia and William 1972).

The specific gravity of fly ash usually ranges from 2.1 to 3.0, while its specific surface area (measured by the Blaine air permeability method) (Annual Book of ASTM Standards) may range from 170 to 1000 m^2/kg.

The color of fly ash can vary from tan to gray to black, depending on the amount of unburned carbon in the ash. The lighter the color, the lower the carbon content. Lignite or subbituminous fly ashes are usually light tan to buff in color, indicating relatively low amounts of carbon as well as the presence of some lime or calcium. Bituminous fly ashes are usually some shade of gray, with the lighter shades of gray generally indicating a higher quality of ash.

2.3.3.2. Chemical Properties

The chemical properties of fly ash are influenced to a great extent by those of the coal burned and the techniques used for handling and storage. There are basically four types, or ranks, of coal, each of which varies in terms of its heating value, its chemical composition, ash content, and geological origin. The four types, or ranks, of coal are

anthracite, bituminous, subbituminous, and lignite. In addition to being handled in a dry, conditioned, or wet form, fly ash is also sometimes classified according to the type of coal from which the ash was derived.

The principal components of bituminous coal fly ash are silica, alumina, iron oxide, and calcium, with varying amounts of carbon, as measured by the loss on ignition (LOI). Lignite and subbituminous coal fly ashes are characterized by higher concentrations of calcium and magnesium oxide and reduced percentages of silica and iron oxide, as well as a lower carbon content, compared with bituminous coal fly ash (Meyers et al. 1976). Very little anthracite coal is burned in utility boilers, so there are only small amounts of anthracite coal fly ash.

Table 2.9 compares the normal range of the chemical constituents of bituminous coal fly ash with those of lignite coal fly ash and subbituminous coal fly ash. From the table, it is evident that lignite and subbituminous coal fly ashes have a higher calcium oxide content and lower loss on ignition than fly ashes from bituminous coals. Lignite and subbituminous coal fly ashes may have a higher concentration of sulfate compounds than bituminous coal fly ashes.

The chief difference between Class F and Class C fly ash is in the amount of calcium and the silica, alumina, and iron content in the ash (Annual Book of ASTM Standards). In Class F fly ash, total calcium typically ranges from 1 to 12 percent, mostly in the form of calcium hydroxide, calcium sulfate, and glassy components in combination with silica and alumina. In contrast, Class C fly ash may have reported calcium oxide contents as high as 30 to 40 percent (McKerall et al. 1982). Another difference between Class F and Class C is that the amount of alkalis (combined sodium and potassium) and sulfates (SO_4) are generally higher in the Class C fly ashes than in the Class F fly ashes.

Table 2.9. Normal range of chemical composition for fly ash produced from different coal types(expressed as percent by weight).

Component	***Bituminous***	***Subbituminous***	***Lignite***
SiO_2	20-60	40-60	15-45
Al_2O_3	5-35	20-30	10-25
Fe_2O_3	10-40	4-10	4-15
CaO	1-12	5-30	15-40
MgO	0-5	1-6	3-10
SO_3	0-4	0-2	0-10
Na_2O	0-4	0-2	0-6
K_2O	0-3	0-4	0-4
LOI	0-15	0-3	0-5

Although the Class F and Class C designations strictly apply only to fly ash meeting the ASTM C618 specification, these terms are often used more generally to apply to fly ash on the basis of its original coal type or CaO content. It is important to recognize that not all fly ashes are able to meet ASTM C618 requirements and that, for applications other than concrete, it may not be necessary for them to do so.

The loss on ignition (LOI), which is a measurement of the amount of unburned carbon remaining in the fly ash, is one of the most significant chemical properties of fly ash, especially as an indicator of suitability for use as a cement replacement in concrete.

CHAPTER 3

MATERIALS AND METHODS

3.1. Sample Preparation and Determination of Size Distribution

The fly ash samples used in this study were obtained from Soma and Yeniköy Power Plants in Turkey. Representative samples of 250 g were obtained by appropriate sampling method. Representative ash samples were placed into a size screen analyzer (Retsch S1000) to determine size distributions of particles.

Adsorbent particle sizes used in adsorption experiments were smaller than 500 μm. The fly ash samples were dried at 105˚C for 2 h before each set of experiments.

3.2. Characterization of Sorbents

Characterization of sorbents was carried out by using X-Ray Diffraction, SEM/EDX analysis, BET analysis and chemical analysis.

3.2.1. SEM, EDX and XRD Analysis

SEM/EDX characterization was carried out using a Philips XL-30S FEG type instrument. Prior to analysis, the solid samples were sprinkled onto Al or C tapes which are adhesive and supported on metallic disks. Images of the sample surfaces were recorded at different magnifications.

X-Ray powder diffraction (XRD) data were collected on a Philips X'Pert Pro diffractometer using Cu Kα radiation (λ=0.154 nm). Samples were prepared by compressing in the cassette sample holder without any adhesive substance.

3.2.2. Surface Area Analysis

All ash samples were analyzed by Micromeritics ASAP 2010 volumetric adsorption device to investigate adsorption properties and porous properties before the batch adsorption studies. Adsorptive gas was nitrogen during the analyses and temperature was constant as 77 K. The working principle of volumetric adsorption measurement device based on monitoring nitrogen gas adsorption (or desorption) on to (from) solid surface at a constant temperature during the interval time. Adsorbed nitrogen gas volume (V_A) as cm^3/g was measured at each pressure, and adsorption isotherms were obtained as a function of V_A and relative pressure (P/P_0). Samples were degassed for a day at 573 K before analyses.

3.2.3. Chemical Analysis

Ash samples were ground to 100 μm for chemical analyses. Firstly, 0.25 g of samples was weighted, 3 g of lithium tetra borate was added into samples, and they were burned at 1100 ^{0}C for 90 minutes. Melting samples were placed in a desiccator, then 100 ml HCl (10 % diluted) was added into samples and they were solved using a magnetic stirrer. Solutions were diluted to 250 ml and their elemental contaminations were determined by an atomic adsorption spectrometer (Perkin Elmer 2280).

3.3. Chemicals and Reagents

Double distilled water which was passed through Barnstead Easypure UV-Compact ultra pure water system (18.3 ohm) was used to prepare all solutions. All reagents were stored in polyethylene-polypropylene containers. Plastic ware were cleaned in dilute nitric acid (10% v/v) and dried at 60˚C after rinsing with deionized water.

Standard boron stock solution (1000 mg/L) was prepared by dissolving 5.716 g anhydrous H_3BO_3 (obtained from the MERCK Chemical Company) in ultra pure water, then diluted to 1000 ml.

Mannitol solution was prepared by dissolving 5.0 g of mannitol in ultra pure water, then diluted to 50 ml.

Lower concentration calibration standards were prepared daily from their stock solutions.

3.4. Instrumentation and Apparatus

In batch adsorption experiments, a temperature-controlled water bath (Nuve ST 402) was employed to adjust temperature. The pH measurements were performed by using InoLab Level 1 pH meter. Boron was determined using a Varian Liberty Series II Axial view ICP-OES throughout the study.

3.5. Determination of Boron

It's reviewed that the most common used analytical methods for the determination of boron in different types of samples are the spectrophotometric methods. These methods have been reported to suffer from several methodological problems and are not adequately sensitive for some water samples that are naturally low in boron concentration. Inductively coupled plasma optical emission spectrometry (ICP–OES) and electro thermal atomic absorption spectrometry (ETAAS) are used most frequently among the atomic spectroscopic methods, although they suffer from interferences, memory effects and insufficient sensitivity for THA determination of low levels of boron. ICP mass spectrometry (ICP–MS) offers higher sensitivity, lower detection limits, and simultaneous measurement of total boron concentration and boron isotope ratios for biological tracer studies in the same run (Kaftan et al. 2004).

The most sensitive emission lines of boron, 249.773 nm and 249.678 nm were chosen to achieve sensitive measurement. 208.959 nm was also chosen incase of Fe interferences (Kaftan 2004).

The most important disadvantage of boron determination with ICP methods is the memory effect of the boric acid. 0.1 M NH_3 and 0.25 % (w/v) mannitol solution were added to all samples and standards to reduce the memory effect as suggested by Kaftan 2004.

3.6. Boron Sorption Studies

In order to find the appropriate sorbent for removal of boron, various adsorbents such as amberlite, zeolite, clay, silica, Yeniköy coal, Yeniköy ash, Soma coal and Soma ash were tested. Initial boron concentrations were 10 mg/L, S/L ratios were 5g/100mL and pH was natural.

3.6.1. Batch Experiments with Yeniköy ash

In batch adsorption experiments known weights of Yeniköy ash (2.5 g) were added to polyethylene tubes containing 50 mL boric acid solution and shaked by a Nuve ST 402 temperature-controlled water bath at approximately 600 rpm (a speed rate at which the ash would not precipitate). The contact time was changed from 2 minutes to 7 days.

The effect of temperature on sorption was examined by operating at various temperatures; 283, 293, 303, 313, 323 and 333 K in a temperature-controlled water bath equipped with a shaker.

Different adsorbent doses (0.625, 1.25, 2.5, 5, 10 and 20 g) were applied to 50 mL of the solution containing 10 mg/L boron at room temperature in order to find out the effect of adsorbent dosage to boron removal.

The effect of initial concentration of boron was examined by studying different initial concentrations changing from 10 to 500 mg/L. Initial concentration values were chosen as 10, 30, 50, 100, 250 and 500 mg/L.

After adsorption, samples were centrifuged at 4600 rpm for 2 minutes. Excess amounts of Ca^{2+} ions were needed to be removed to prevent damaging to the torch of the ICP. For this reason, 40 mL of supernatants were taken and Ca^{2+} ions were precipitated by adding 0.568 g of di-ammonium oxalate monohydrate (extra pure $\geq$ 99 %, MERCK product). Required amount of oxalate was calculated from the equation below:

$$Ca^{2+} + (NH_4)_2C_2O_4 \rightarrow CaC_2O_4 + 2NH_4^+$$

The contents were filtered with syringe filters (0.45μm, Sartorius Minisart RC 25). After addition of ammonia and mannitol, boron was determined by using ICP-OES.

3.6.2. Effect of pH on Sorption

In aqueous solutions, fly ash reacts with water and produces varying salinity and compositions depending on the solid/liquid ratio, extraction time and temperature. The final pH of the solution depends on the content of the basic oxides and the amount of acidic substances such as SO_2, SO_3 and P_2O_5, which are also present in the coal fly ash. Among strong basic oxides in the combustion product CaO undergoes the largest variation and therefore the CaO content is the best indicator of the alkaline or neutral reaction.

pH of the solutions was measured between 11.8 and 13 during the experiments and couldn't be controlled because of ash's natural buffer behavior. For this reason all experiments were performed under natural pH conditions and boron was found as borate anion during sorption experiments.

3.7. Determination of Water Quality

3.7.1. Leaching of Ash

Leaching of ash was determined using the Standard Method ASTM D-4793. Ash samples were placed in double distilled water (S/L= 0.05) at natural pH and shaken on an IKA Labortech-KS125 digital shaker for 24 hours at room temperature with 600 rpm mixing speed. To withdraw liquid from suspensions, a series of Macherey Norgel type (40x40) filter paper with a vacuum system and syringe filters from Sartorius Minisart RC 25, 0.45 μm were utilized. The supernatant solutions were analyzed by an ICP (Inductively Coupled Plasma-Atomic Emission Spectrophotometer) from Varian, AES Axial Liberty Series 2. 0.2 ml of nitric acid was added into each supernatant solution (20 ml) to prevent sedimentation of heavy metals and major elements before the multielement analysis. Multielement stock solution (ICP multielement standard solution IV from MERCK Company; 1000 mg/L Ag, Al, B, Ba, Bi, Ca, Cd, Co, Cu, Fe, Ga, In, K, Li, Mg, Mn, Na, Ni, Pb, Sr, Tl, Zn) prepared daily at least three different concentration for each time to get calibration curves.

CHAPTER 4

RESULTS AND DISCUSSION

4.1. Characterization Results of Ash

4.1.1. Determination of Size Distribution

Figure 4.1 illustrates the cumulative particle size distributions of Soma and Yeniköy fly ash samples after screen analyses. The nominal particle size values k_1 and k_2 were found to be 100 and 165 μm for Yeniköy and Soma fly ashes respectively. 100% of all ash samples were under 500 μm and adsorption experiments were carried out using particle sizes below 500 μm.

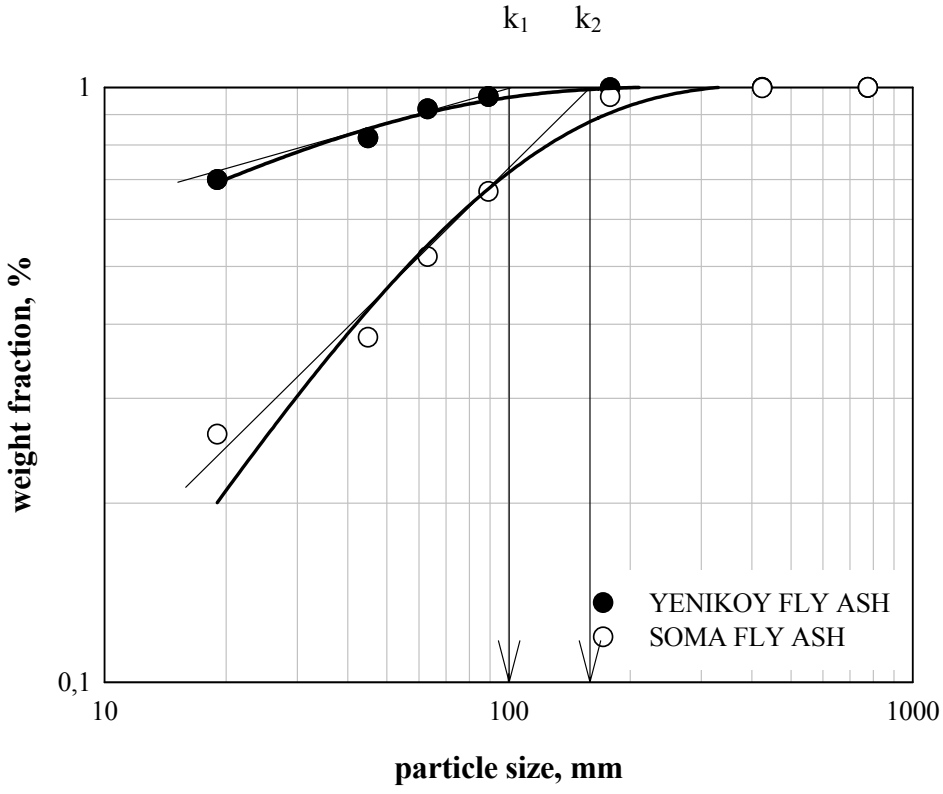

Figure 4.1. Cumulative particle size distribution of Yeniköy and Soma Fly Ash

4.1.2. SEM, EDX and XRD Analyses

Ash samples were characterized and analyzed to obtain their mineralogical and elemental constituents using XRD and SEM/EDX techniques. The XRD diagrams of two kinds of ashes are shown in Figure 4.2 and 4.3. X-ray diffraction studies revealed the presence of labradorite, portlandite, anhydrite, larnite, lime and quartz minerals in the ash samples. The mineralogical composition of each of the two ash samples is summarized in Table 4.1.

Table 4.1. XRD Analyses of Lignite Samples

Soma Ash	**Yeniköy Ash**
Labradorite	Larnite
Portlandite	Portlandite
Anhydrite	Anhydrite
Quartz	Quartz
Lime	Lime

EDX results of the atomic percentages of N, O, Mg, Al, Si, S, K, Ca, Ti, Fe and molecular percentages of their oxides in both ash samples were obtained by spot analysis. Many points were randomly selected on the surface of samples and a mean value was calculated for each element or compound. A summary of the EDX results with the corresponding standard deviations are given in Table 4.2 and 4.3. According to this analysis, Soma ash is seen to be richer in the oxides of Si, Ca and Al, while Yeniköy ash is mainly composed of Ca and S oxides.

The standard deviations can be used as an indicator of the surface heterogeneity of the ash samples. It must be noted also that for the elements present below 5%, the error inherited in the EDX measurement can rise up to more than 50%. Moreover, it is important to keep in mind that the EDX information stands for the upper few micrometers of the surface of ash samples.

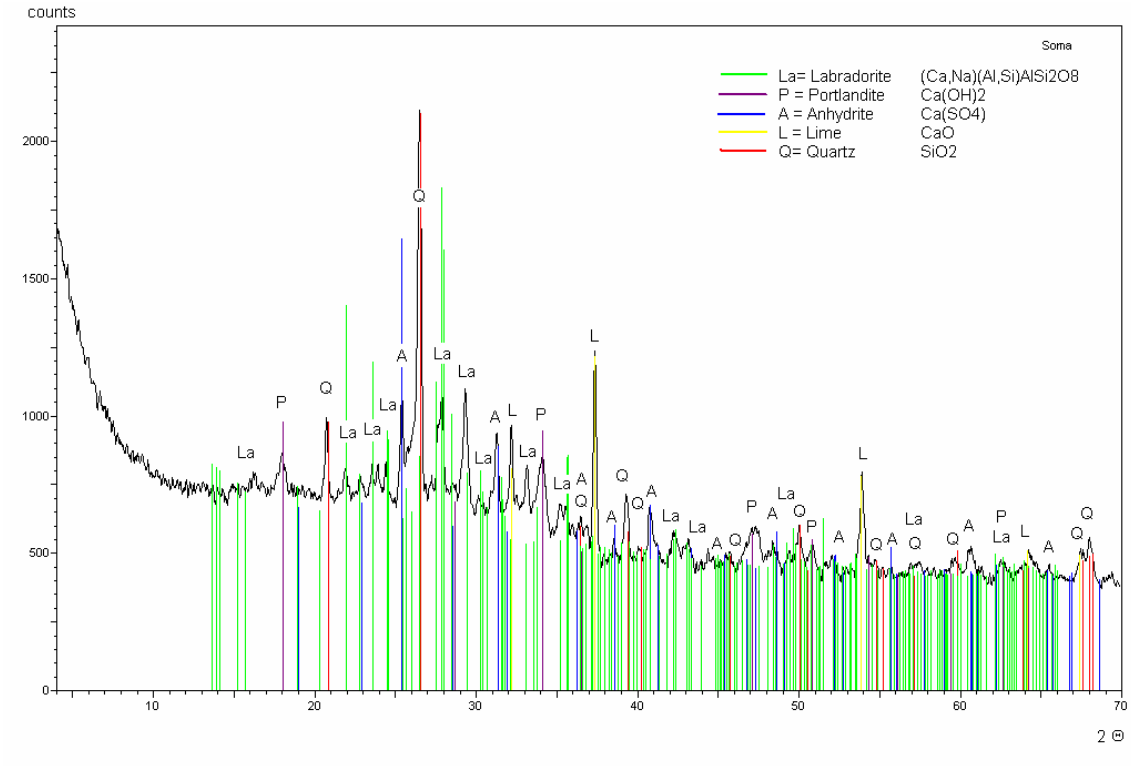

Figure 4.2. XRD diagram of Soma ash

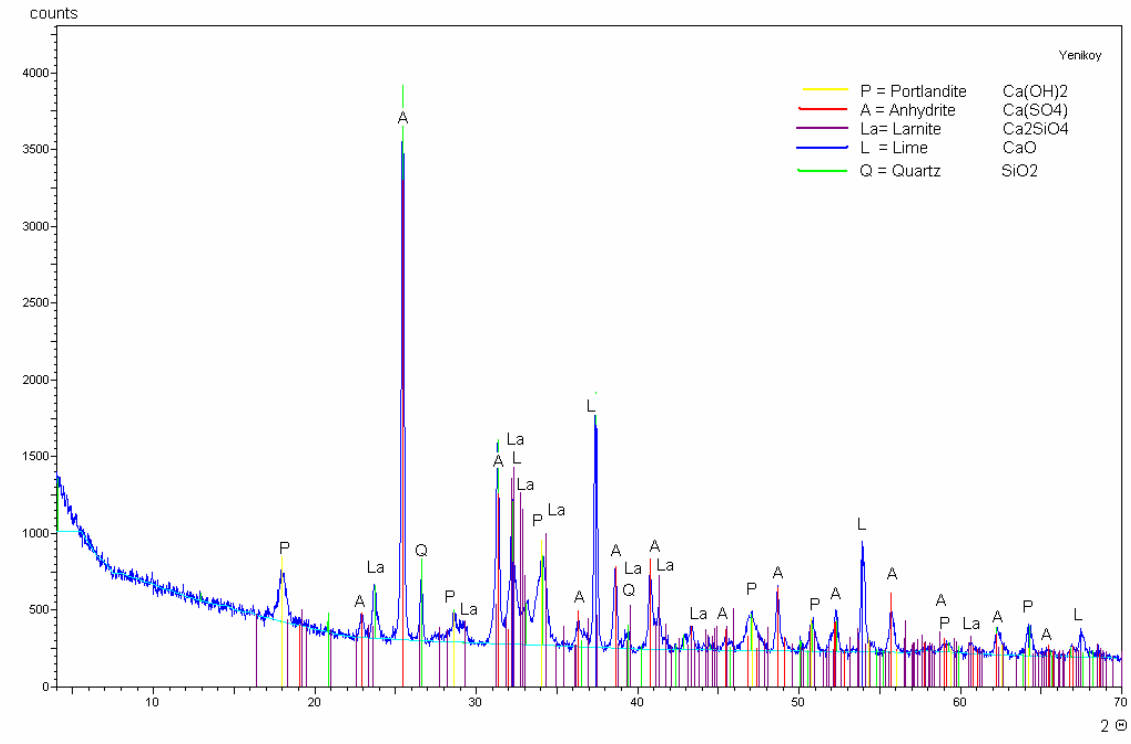

Figure 4.3. XRD diagram of Yeniköy ash

Table 4.2. EDX results of atomic percentages

Sample	Element	% At 1	% At 2	% At 3	% At 4	% At 5	% At 6	% At 7	% At 8	Mean	± S.D.
Soma Ash	N	9.27	11.23	16.80	13.56	16.63	13.36	11.93	11.58	13.05	2.63
	O	54.89	58.84	60.96	55.67	58.01	59.85	54.27	54.96	57.18	2.56
	Mg	1.31	0.97	0.44	0.79	0.59	0.95	0.97	1.11	0.89	0.28
	Al	9.13	7.59	0.85	4.18	1.66	2.36	4.43	12.14	5.29	3.97
	Si	13.12	12.31	1.03	5.94	1.76	5.92	8.44	16.26	8.10	5.47
	S	0.65	0.67	0.97	1.27	0.34	0.54	2.80	0.21	0.93	0.83
	K	0.98	0.75	0.29	0.63	0.36	0.46	0.96	0.69	0.64	0.26
	Ca	8.38	6.56	18.18	17.49	20.30	15.71	15.24	2.08	12.99	6.49
	Ti	0.28	0.23	0.00	0.00	0.00	0.09	0.18	0.11	0.11	0.11
	Fe	1.99	0,85	0.49	0.46	0.34	0.76	0.79	0.84	0.82	0.51
Yeniköy Ash	N	0.00	13.41	11.94	8.70	12.42	15.80	13.95	11.06	10.91	4.88
	O	61.46	53.33	57.96	56.10	62.81	58.71	51.23	54.61	57.03	3.98
	Mg	0.78	1.31	0.49	1.73	0.65	0.75	0.30	0.19	0.78	0.52
	Al	2.11	1.90	1.09	1.65	1.48	1.87	0.65	1.22	1.50	0.49
	Si	2.66	2.78	0.46	2.31	1.54	2.46	0.99	1.30	1.81	0.86
	S	9.12	6.81	10.68	6.63	4.20	5.50	3.30	11.95	7.27	3.07
	K	0.00	0.00	0.00	0.00	0.00	0.00	0.00	0.00	0.00	0.00
	Ca	23.02	19.64	17.02	22.05	16.17	14.68	29.23	19.04	20.11	4.65
	Ti	0.09	0.00	0.03	0.00	0.00	0.00	0.00	0.06	0.02	0.03
	Fe	0.75	0.82	0.33	0.84	0.72	0.23	0.35	0.59	0.58	0.24

Table 4.3. EDX results of molecular percentages

Sample	Element	% Mol 1	% Mol 2	% Mol 3	% Mol 4	% Mol 5	% Mol 6	% Mol 7	% Mol 8	Mean	± S.D.
Soma Ash	N_2O_5	12.12	16.88	27.47	17.94	24.47	20.34	14.59	15.85	18.71	5.14
	MgO	3.93	3.22	1.49	2.32	1.85	3.04	2.74	3.65	2.78	0.85
	Al_2O_3	13.63	12.57	1.43	6.15	2.59	3.77	6.23	19.62	8.25	6.37
	SiO_2	38.58	40.34	3.50	17.34	5.51	18.87	23.51	50.96	24.83	17.05
	SO_3	1.89	2.18	3.29	3.69	1.06	1.72	7.73	0.64	2.78	2.25
	K_2O	1.44	1.23	0.49	0.92	0.57	0.73	1.33	1.09	0.98	0.36
	CaO	24.64	21.44	61.49	50.97	63.41	50.03	42.27	6.51	40.10	20.49
	TiO_2	0.82	0.76	0.00	0.00	0.00	0.30	0.51	0.35	0.34	0.33
	Fe_2O_3	2.94	1.39	0.83	0.67	0.53	1.21	1.09	1.33	1.25	0.75
Yeniköy Ash	N_2O_5	0.00	15.52	15.37	10.56	20.47	22.76	15.38	12.51	14.07	6.91
	MgO	2.10	3.51	1.42	4.59	2.19	2.40	0.75	0.50	2.18	1.37
	Al_2O_3	2.84	2.53	1.57	2.19	2.49	2.98	0.81	1.62	2.13	0.74
	SiO_2	7.17	7.39	1.33	6.09	5.17	7.82	2.46	3.44	5.11	2.45
	SO_3	24.57	18.05	30.84	17.48	14.13	17.40	8.16	31.47	20.26	8.11
	K_2O	0.00	0.00	0.00	0.00	0.00	0.00	0.00	0.00	0.00	0.00
	CaO	62.05	51.92	48.90	57.98	54.33	46.28	72.02	49.56	55.38	8.45
	TiO_2	0.26	0.00	0.09	0.00	0.00	0.00	0.00	0.15	0.06	0.10
	Fe_2O_3	1.02	1.08	0.47	1.11	1.21	0.36	0.42	0.76	0.80	0.35

SEM microimages were recorded to reveal the morphology of the ash samples. Typical SEM images of samples are given in Figure 4.4 and 4.5.

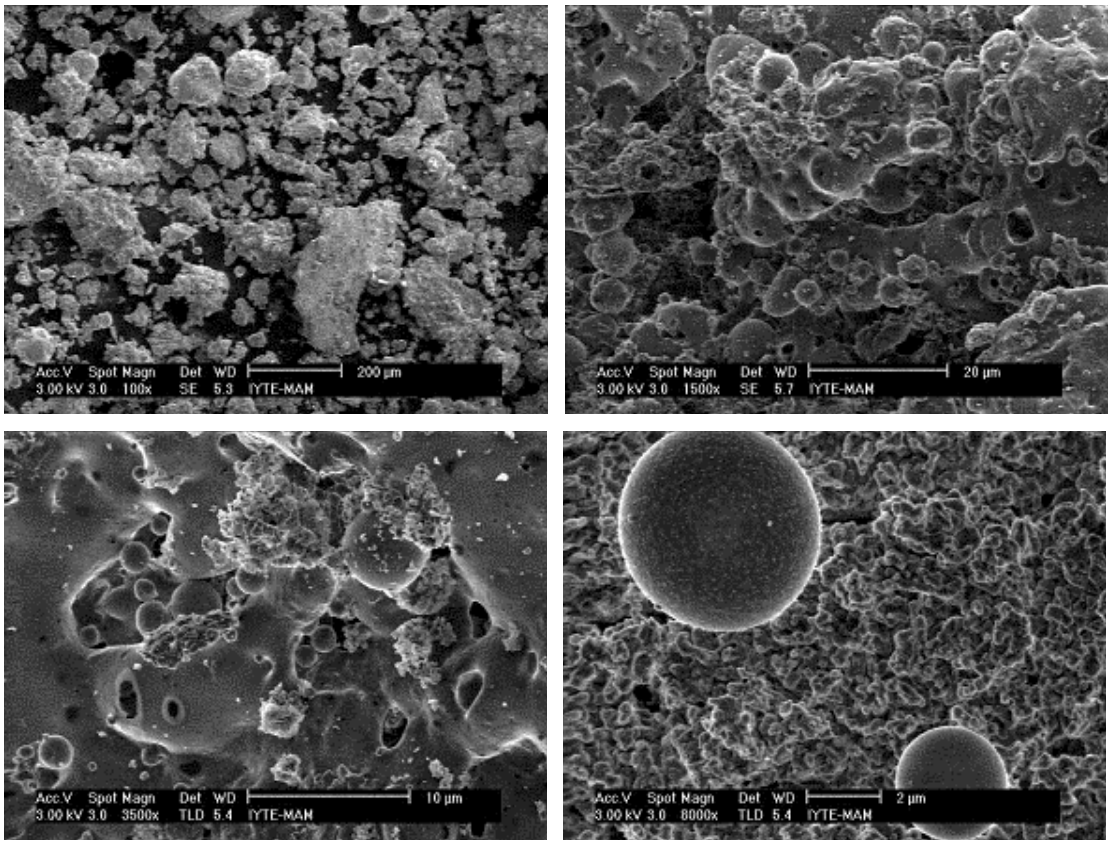

Figure 4.4. SEM images of Soma fly ash

The SEM analysis indicated structural differences among both types of fly ash samples. For Soma ash (Fig.4.4), the microscopic image shows agglomerations of irregular shape accompanied by a few rather smooth spherical particles. The surface of the agglomerations reveals many small channels. In the third picture there is a relatively large particle of rough surface and many inner channels of about 2 μm diameter.

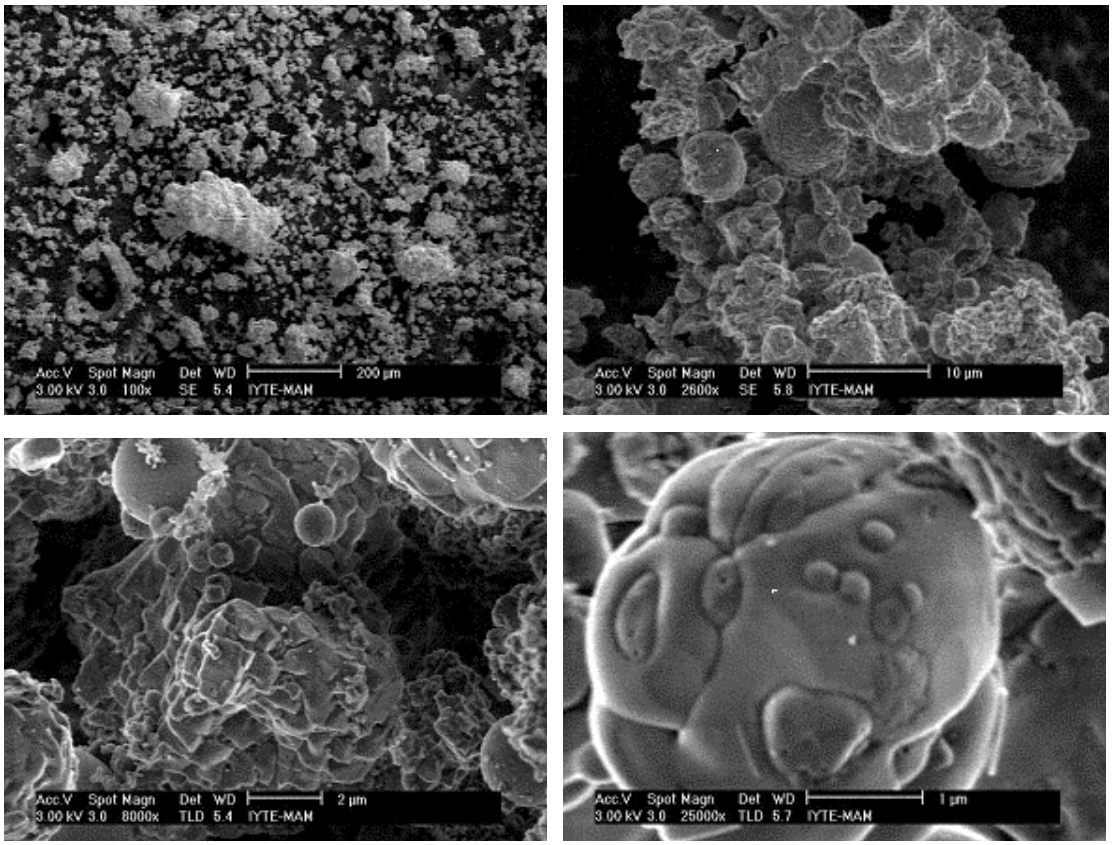

Figure 4.5. SEM images of Yeniköy fly ash

The microscopic images of Yeniköy ash reveal the presence of sporadically particles of irregular size. Amount of spherical particles appeared to be less than that observed in Soma ash and agglomeration of rough particles is mostly observed. Roughness of the surface of Yeniköy ash seems to be greater than that of Soma ash. This could be the reason for a few times greater surface area of Yeniköy ash relative to Soma ash as shown in the next section.

4.1.3. Surface Area Analysis

The properties related to the texture of fly ashes are presented in Table 4.4. The surface area of the samples was determined by the BET method and Langmuir method.

Table 4.4. Surface area analysis results of fly ashes

Fly ashes	Surface area (m^2/g)		Micropore area (m^2/g), t-method	Average pore diameter (Å), BET	Pore Volume (cm^3/g), t-method
	BET	Langmuir			
Soma	9.6	13.8	7.2	25.8	0.004
Yeniköy	25.2	35.3	11.1	30.1	0.006

It was found that the surface area of Yeniköy fly ash is almost three times greater than the surface area of Soma fly ash. Yeniköy ash contains pores of larger volume as can be seen in Table 4.4 the thing that is evidenced by a high increase of nitrogen adsorption at a very low relative pressure P/P_0 (Figure 4.6).

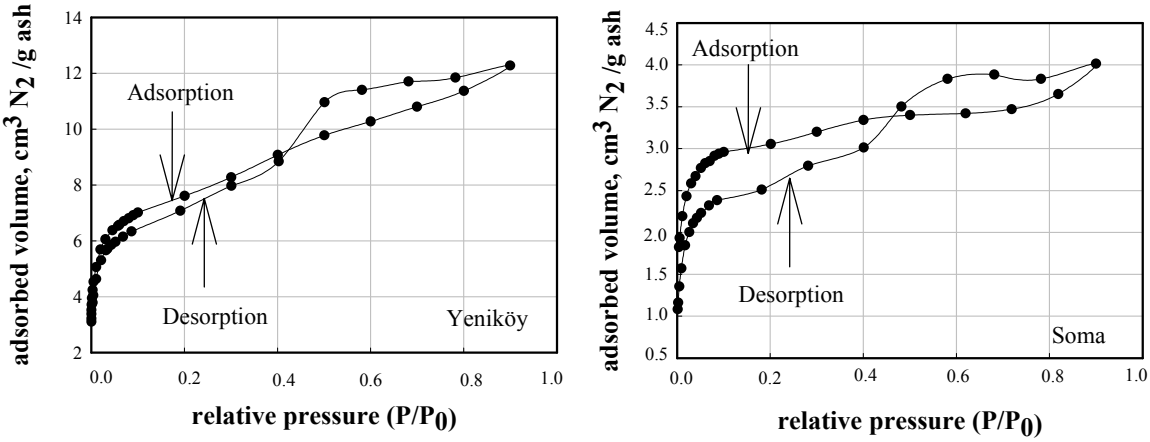

Figure 4.6. N_2 adsorption isotherms for ash samples

A summary of characterization results obtained from EDX and BET analysis is presented below in Table 4.5.

Table 4.5. Characteristic properties of ash samples

Elements, % At			Oxides, % Mol			Physical Properties		
	Soma	**Yeniköy**		**Soma**	**Yeniköy**		**Soma**	**Yeniköy**
N	13.05	10.91	N_2O_5	18.71	14.07	BET surface area, m^2/g	9.6	25.2
O	57.18	57.03	MgO	2.78	2.18	Langmuir surface area, m^2/g	13.8	35.3
Mg	0.89	0.78	Al_2O_3	8.25	2.13	Average pore diameter, Å	25.8	30.1
Al	5.29	1.5	SiO_2	24.83	5.11	Pore volume, cm^3/g	0.004	0.006
Si	8.1	1.81	SO_3	2.78	20.26	Nominal particle size, mm	165	100
S	0.93	7.27	K_2O	0.98	0	Micropore area, m^2/g	7.2	11.1
K	0.64	0	CaO	40.1	55.38			
Ca	12.99	20.11	TiO_2	0.34	0.06			
Ti	0.11	0.02	Fe_2O_3	1.25	0.8			
Fe	0.82	0.58						

4.2. Effect of Parameters on Adsorption

Various operational parameters were tested in order to determine the feasibility of using fly ash materials for boron removal from aqueous solutions. These include time of reaction, material type, solid/liquid (S/L) ratio, temperature and boron concentration.

4.2.1. Effect of Material Type

Batch experiments were carried out for 24 hours at 298 K to evaluate the effect of material type on boron removal from aqueous solutions (initial boron concentration: 10 mg/L; pH: natural, S/L: 0.05). The materials tested were amberlite IRA 743, natural zeolite rich in clinoptilolite, clay, silica, Yeniköy coal, Yeniköy ash and Soma ash. The results are presented in Figure 4.7. The magnitude of boron removal reaches to almost 99% for amberlite and Yeniköy ash samples, while other samples under the similar experimental conditions yield only 30% removal. As seen in Figure 4.7, the ability of Yeniköy fly ash to remove boron is similar to that achieved by amberlite. Therefore, Yeniköy ash was selected for sorption studies.

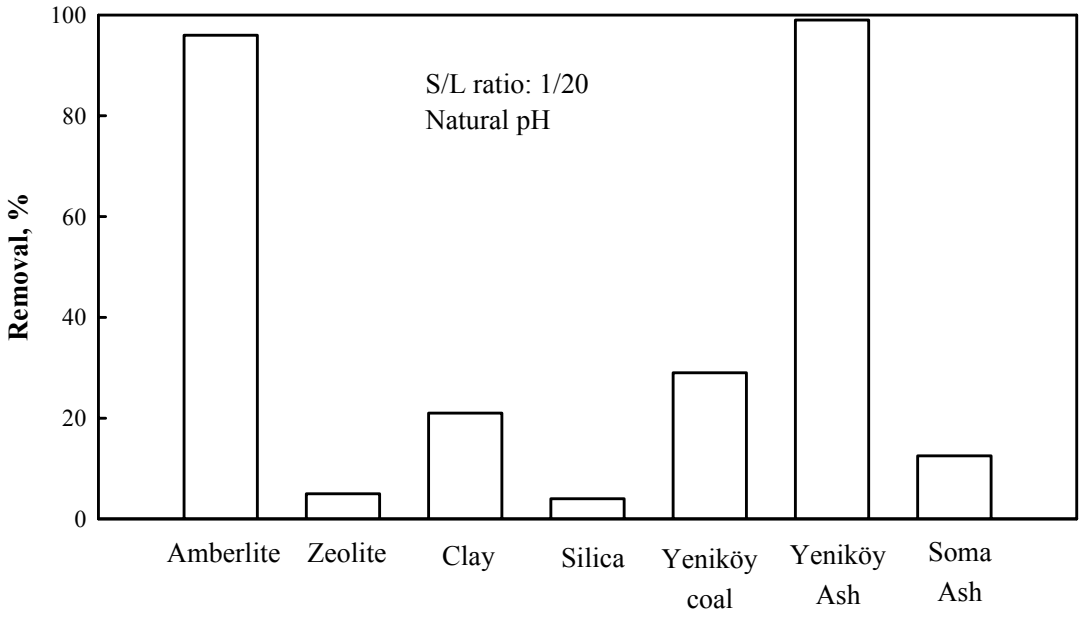

Figure 4.7. Effect of material type on the removal of boron (initial boron concentration: 10 mg/L; pH: natural, temperature: 298 K, S/L: 0.05, mixing time: 24 hours)

4.2.2. Effect of Solid / Liquid Ratio

The effects of solid/liquid ratio for Soma and Yeniköy ashes were examined at S/L ratios of 1.25/100, 2.5/100, 5/100, 10/100, 20/100 and 40/100 mg/L. In these experiments, operational parameters were kept constant (T=298 K, C_0=10 mg/L, pH= natural). The results are presented in Figures 4.8 and 4.9. Generally, it is observed that boron removal increases with increasing solid/liquid ratios for Yeniköy ash and Soma ash.

The tri-dimensional plots were also constructed to better reveal the effect of S/L ratio (Figure 4.10). As it is seen after a certain time and S/L ratio boron removal reaches up to 70% removal.

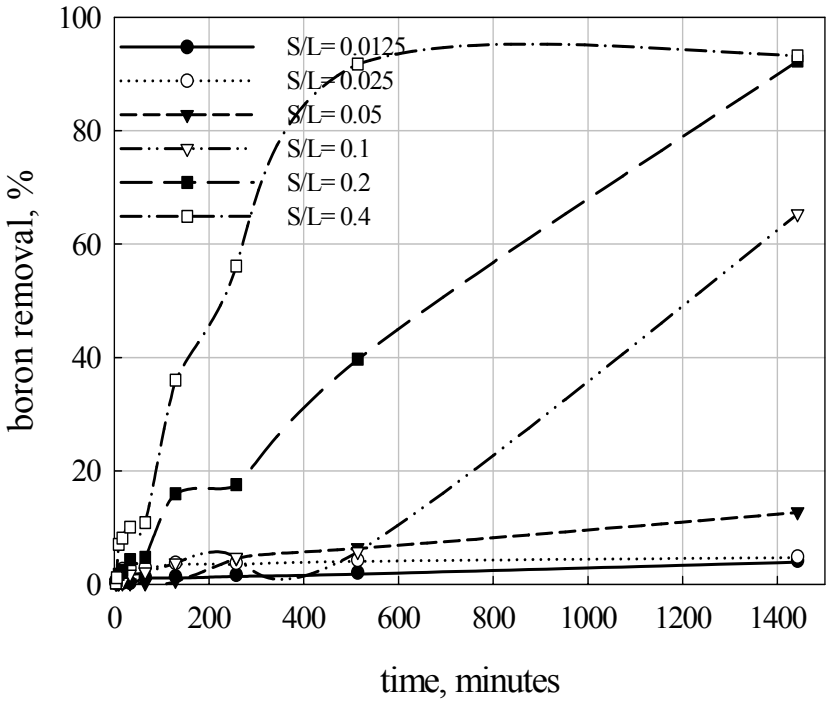

Figure 4.8. Effect of S/L ratio on adsorption of boron for Soma fly ash (initial boron concentration: 10 mg/L; pH: natural; temperature: 298 K; 24 hours)

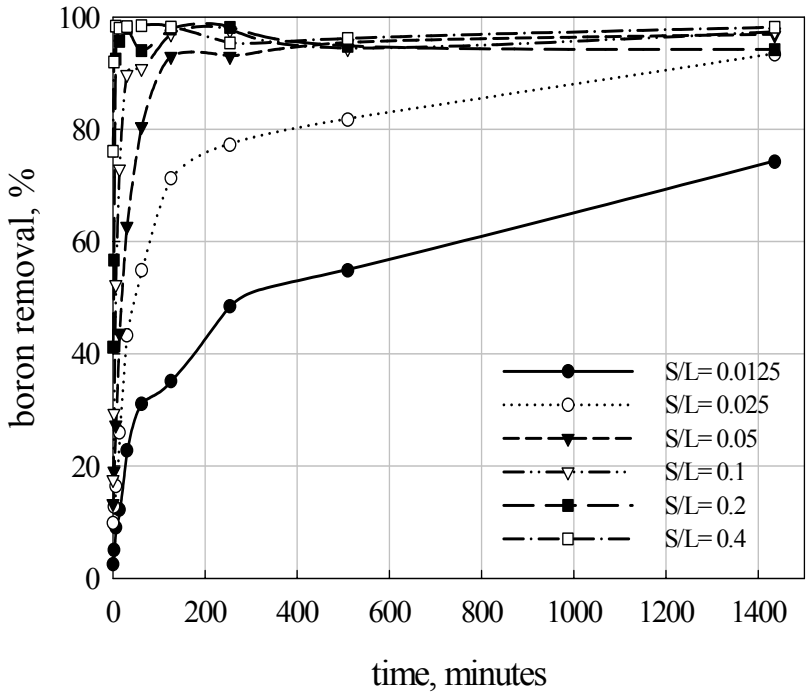

Figure 4.9. Effect of S/L ratio on adsorption of boron for Yeniköy fly ash (initial boron concentration: 10 mg/L; pH: natural; temperature: 298 K)

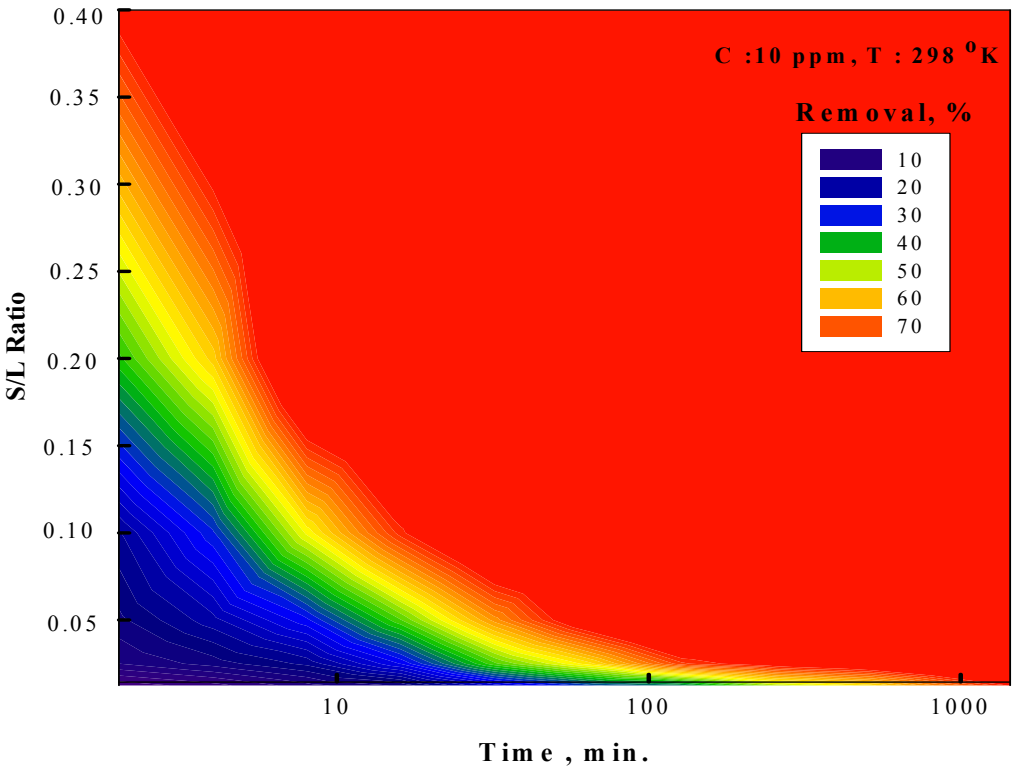

Figure 4.10. Removal of boron as a function of S/L ratio and time for Yenikoy fly ash (initial boron concentration: 10 mg/L; pH: natural; temperature: 298 K)

Increasing solid/liquid ratio leads to an increase in the number of active sites available for adsorption and thus fixation of a larger amount of the solute ions as long as an enough number of these ions is available in the solution in contact with the solid.

Moreover, it is interesting to see that for Soma ash, at a solid/liquid ratio of 0.4 (Figure 4.8), the boron species are almost totally removed within a relatively shorter period of time, the thing probably attributed to the availability of an excess of the accessible adsorption sites at such S/L in a way that minimizes the competition between boron species for a particular available site.

On the other hand, the Yeniköy fly ash, which was shown previously to possess larger pore volume and surface area as compared to Soma fly ash, is able to reach nearly a 100 % removal of boron even at solid/liquid ratio of 0.05. This practically means that smaller amounts of Yeniköy fly ash, about one tenth that of Soma fly ash, would be enough to remove a given amount of aqueous boron at equivalent time periods.

4.2.3. Effect of Time

The kinetic studies of sorption were carried out for different initial concentrations of 10, 30, 50, 100, 250 and 500 mg/L of boron on Yeniköy fly ash. The variation of the sorbed amounts of boron on ash at temperatures of 298, 308 and 318 is presented in Figure 4.11. As seen in the plots, equilibrium of sorbed boron on ash was achieved with the lower concentrations of 10, 30 and 50 mg/L. At high concentrations (100, 250 and 300 mg/L), a period of 7 days is not enough to attain equilibrium.

The time needed to reach equilibrium is generally observed to increase with increasing temperature. This could be suggesting an enhancement in the desorption steps by destabilizing the adsorbed boron specie as temperature is raised.

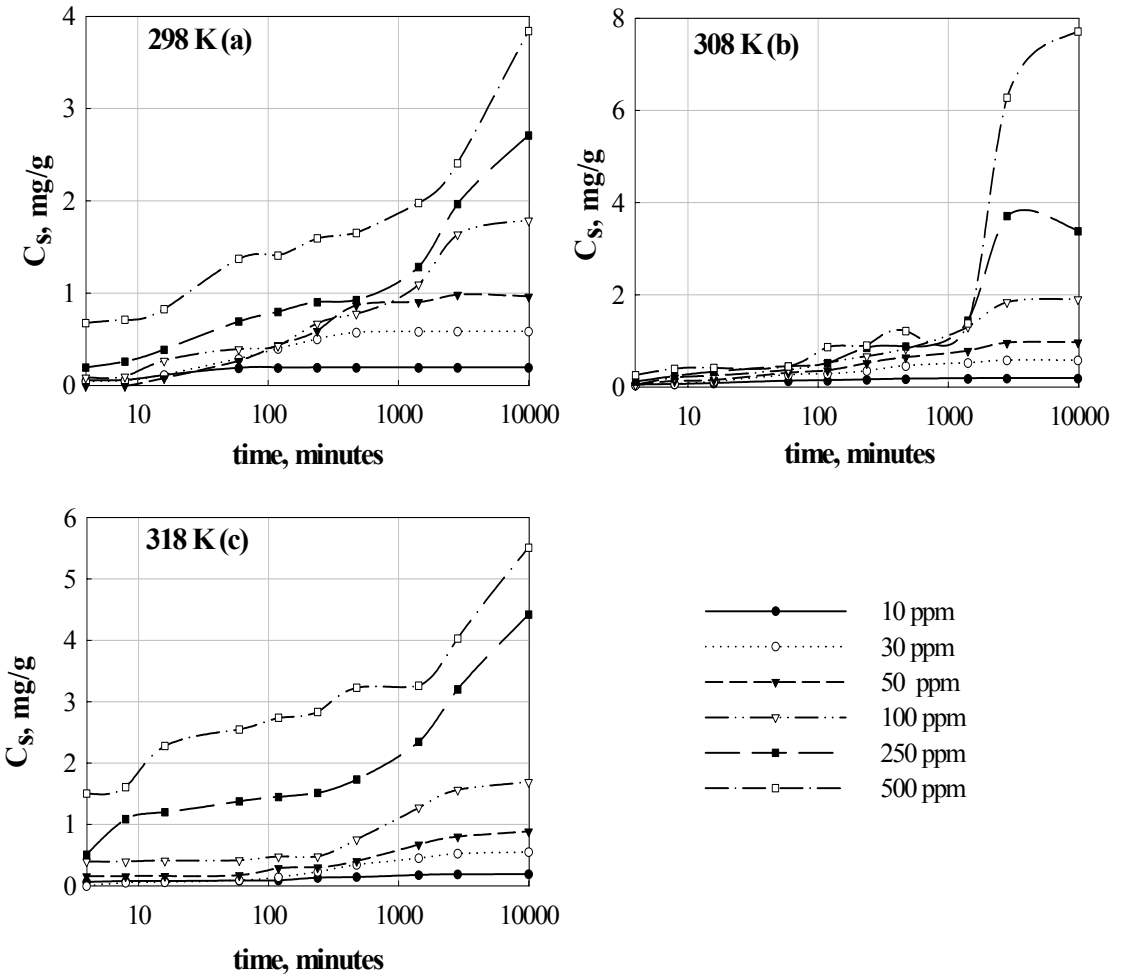

Figure 4.11. Variation of the sorbed amounts of boron on Yeniköy fly ash with time at 298 (a), 308 (b) and 318 K (c) (S/L=0.05, pH: natural)

4.2.3.1. Determination of Rate Parameters

The variation of the adsorbed boron with time was kinetically characterized using the pseudo-first-order equation proposed by Lagergren (Singh et. al., 2005), the pseudo-second-order equation proposed by Ho (Ho and McKay, 2000; Kannan and Sundaram, 2001) and the intraparticle diffusion model (Crank, 1933).

$$log(q_e-q_t) = log(q_e) - k_1 t/2.303 \quad (4.1)$$

$$t/q_t = 1/(k_2 q_e^2) + t/q_e \quad (4.2)$$

$$q_t = k_p t^{1/2} + C, \quad (4.3)$$

where q_t and q_e are the amount of boron adsorbed (mg/g) at time t and at equilibrium time, respectively, k_1 is the pseudo-first-order rate constant for the boron adsorption process (min^{-1}), k_2 is the pseudo-second-order rate constant ($g*mg^{-1}*min^{-1}$), k_p is the intraparticle diffusion rate constant ($mg/g*min^{1/2}$), and C is the intercept of the line which is proportional to the boundary layer thickness.

$log(q_e-q_t)$ was plotted versus t to test whether the sorption data obey the pseudo-first-order kinetics. On the other hand, the equilibrium rate constants of pseudo-second-order were determined by plotting t/q_t against t. The equilibrium rate constants of intraparticle diffusion were also determined by plotting q_t against $t^{1/2}$. The values of these constants were calculated for 10, 30 and 50 mg/L because equilibrium was approached at these concentrations. High concentrations of boron (100, 250 and 500 mg/L) did not attain equilibrium within 7 days and were not thus included in the kinetic analysis.

The kinetic constants and correlation coefficients of these models were calculated and are given in Table 4.6. Better correlation coefficients were obtained from the pseudo-second-order fits as compared to pseudo-first-order kinetics. The plots of the adsorption data using the pseudo-second-order-model are demonstrated in Figure 4.12.

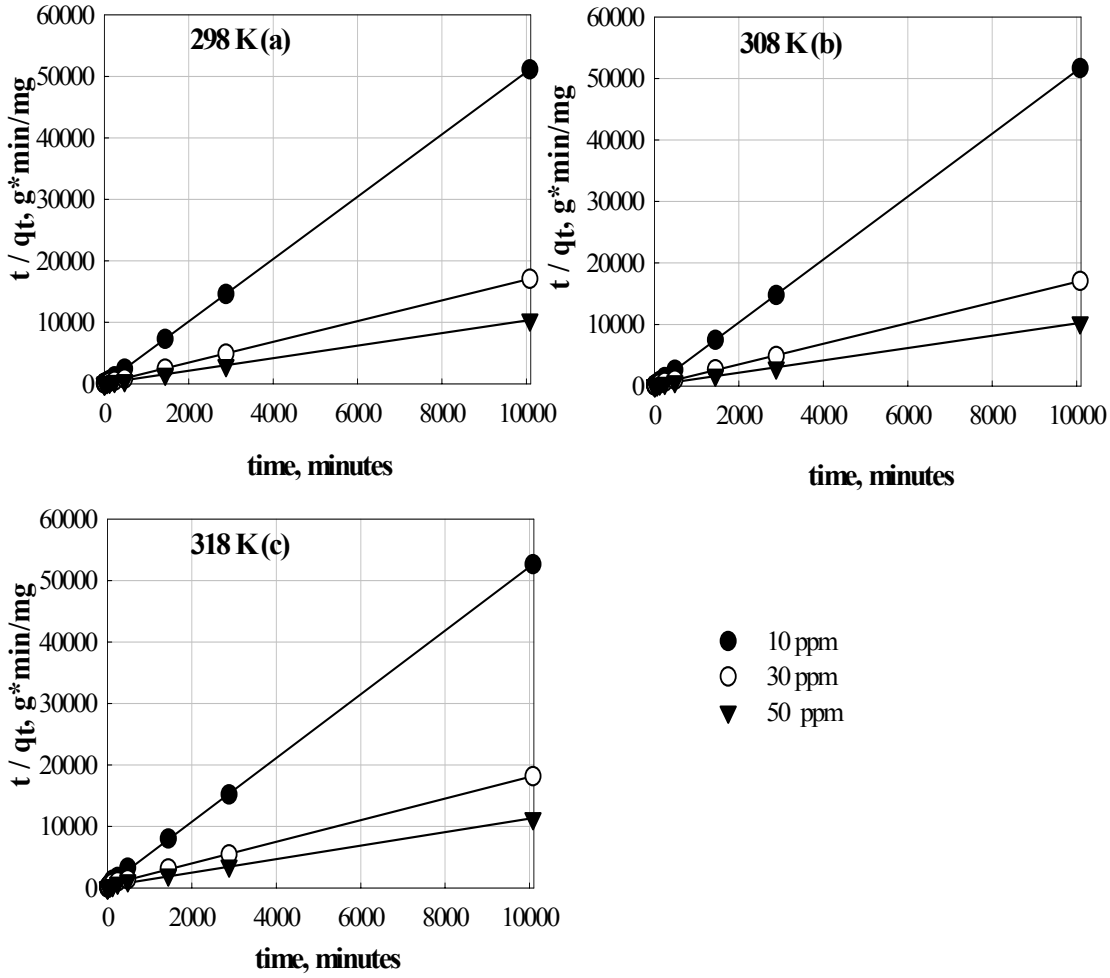

Figure 4.12. Second-order kinetic plots for the adsorption of boron onto Yeniköy fly ash

Table 4.6. A comparison of kinetic model rate constants obtained under different conditions

T (K)	C_0 (mg/L)	k_1 (min^{-1})	R_1	k_2 ($g/mg^{-1}*min^{-1}$)	R_2	k_p ($mg/g^{-1}*min^{-1/2}$)	R_p
298	**10**	0.011	0.793	0.862	1.000	0.025	0.988
	30	0.008	0.999	0.037	1.000	0.036	0.987
	50	0.005	0.995	0.008	1.000	0.044	0.997
308	**10**	0.005	0.956	0.213	1.000	0.015	0.998
	30	0.003	0.972	0.018	1.000	0.039	0.999
	50	0.002	0.974	0.006	0.999	0.031	0.994
318	**10**	0.002	0.964	0.069	1.000	0.003	0.955
	30	0.002	0.996	0.007	0.999	0.010	0.971
	50	0.001	0.972	0.004	0.998	0.013	0.992

It is important to notice that the values of the rate constant, k_2, decrease as temperature is increased. This means that, regardless of the amount adsorbed, equilibrium attainment will be delayed as temperature is raised. Based on the behavior of gases, it is expected that the rate constant would increase as temperature increases, due to the increase in the kinetic energy of molecules/atoms that usually lack effective interactions in between them in the gaseous phase (Levine 2002). In solution-solid interactions, however, the situation is more complex and the nature of interionic (or intermolecular) forces is much different. Other authors have also reported the decrease in k_2 with increase in temperature (Al-Ghouti et.al. 2005).

The sorption process of solutes in solution onto porous solid is known to involve bulk transport, then intraparticle diffusion followed by the fixation step of the solute by the sorption site. The intraparticle diffusion model is applied to test whether bulk transport or intraparticle diffusion is the rate determining step. The corresponding plots are shown in Figure 4.13.

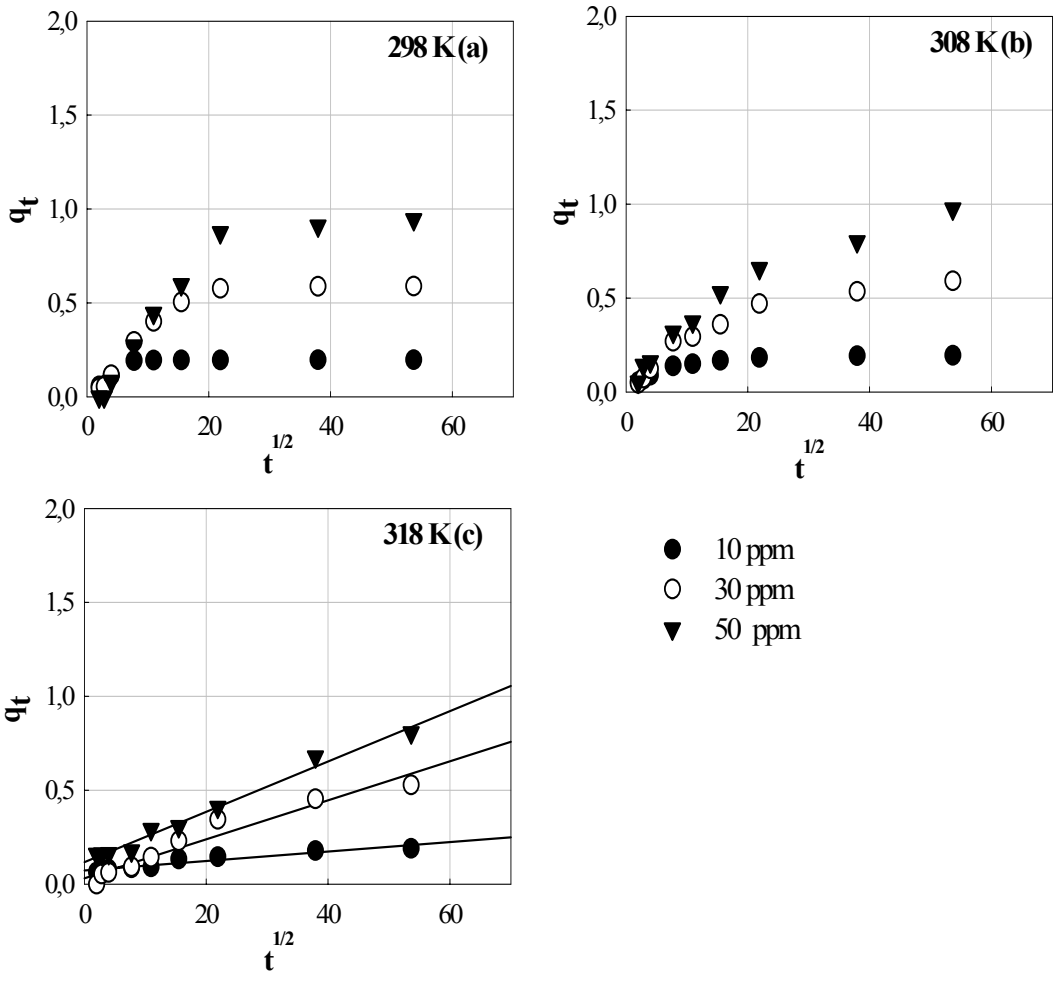

Figure 4.13. Intraparticle diffusion plots for the adsorption of boron onto Yeniköy ash

If the intraparticle diffusion is involved in adsorption process, a plot of $t^{1/2}$ versus q_t would result in a linear relationship, and the particle diffusion would be the controlling step if this line passed through the origin. Moreover, if the extrapolated lines of the data at the initial sorption stages do not pass through the origin, then this would be indicative of some degree of boundary layer control (Özcan and Özcan. 2004). In this study, the results indicate that the intraparticle diffusion is possibly not the rate controlling step, and that other process may be taking part in the control of the rate of adsorption; e.g. external mass transport.

4.2.3.2. Determination of Activation Energy

The activation energy refers to the minimum kinetic energy that must be supplied to the system in order for a chemical process to take place. Arrhenious equation which relates the apparent rate constant with the reaction temperature is given as

$$ln\ k = ln\ A - (\ E_a / RT\ ) \qquad (4.4)$$

where, k is the pseudo-second-order rate constant, A is the pre-exponential factor or frequency factor which can be calculated as exp(intercept), E_a is the activation energy and can be directly calculated from the slope of the lnk versus $1/T$ plot and R is the perfect gas constant (8,3145 J/mole K). The data in Table 4.7 was plotted in this form in Figure 4.14. The obtained results for the "apparent" activation energies were negative. This is due to the fact that the rate constant decreases when temperature is increased as mentioned previously. The tabulated values suggest that as the initial concentration increases, the effect of temperature, as a delaying factor for sorption, will decrease. This observation is reflected in E_a, the absolute values of which decreases with increase in initial concentration. From the values of A, it can be concluded that the fraction of boron species possessing an energy enough to overcome the activation energy barrier increases as the initial concentration is raised.

Table 4.7. The kinetic parameters obtained from the linear fits of the experimental data to the second order rate equation

C_0 (mg/L)	T (K)	k_2 (g/mg^{-1}*min^{-1})	q_e (mg/g)	R_2	E_a (kJ/mole)	A
10	298	0.862	0.197	1.000	-99,6	2.96 x 10 $^{-18}$
	308	0.213	0.196	1.000		
	318	0.069	0.193	1.000		
30	298	0.037	0.593	1.000	-67,1	6.77 x 10 $^{-14}$
	308	0.018	0.596	1.000		
	318	0.007	0.568	0.999		
50	298	0.008	0.983	1.000	-26,9	1.62 x 10 $^{-7}$
	308	0.006	0.995	0.999		
	318	0.004	0.910	0.998		

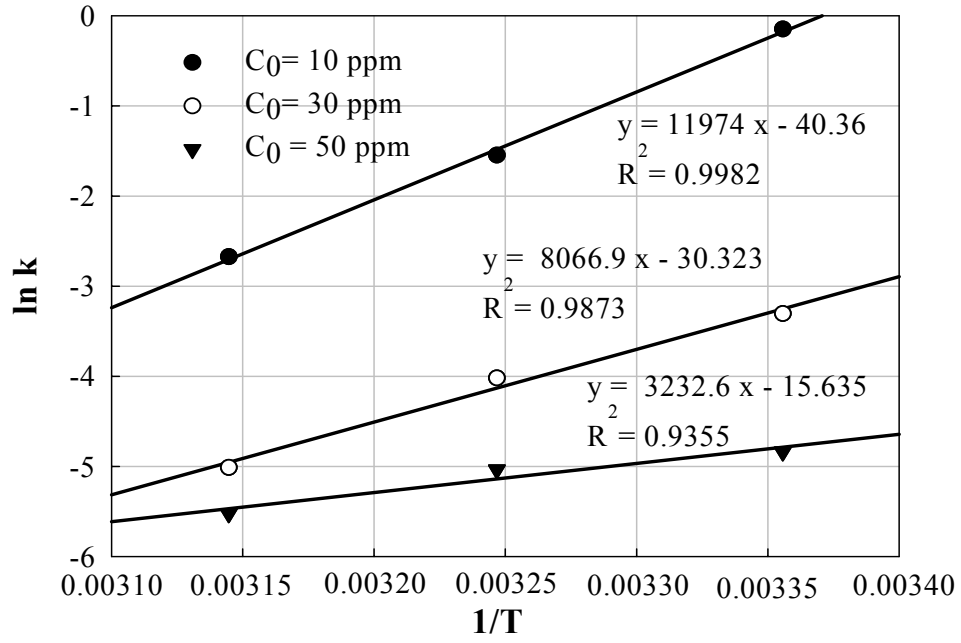

Figure 4.14. Linear regration of 1/T vs. ln k calculated from Arrhenius Equation.

4.2.4. Effect of Concentration and Temperature

A series of experiments were performed at different initial adsorbate concentrations, viz., 10, 30, 50, 100, 250 and 500 mg/L, at temperatures of 298, 308 and 318 K and natural pH.

The results are given in Figure 4.15. It can be seen that increasing the initial concentration is accompanied by a decrease in the percentage adsorption of boron and causing a delay in the attainment of equilibrium.

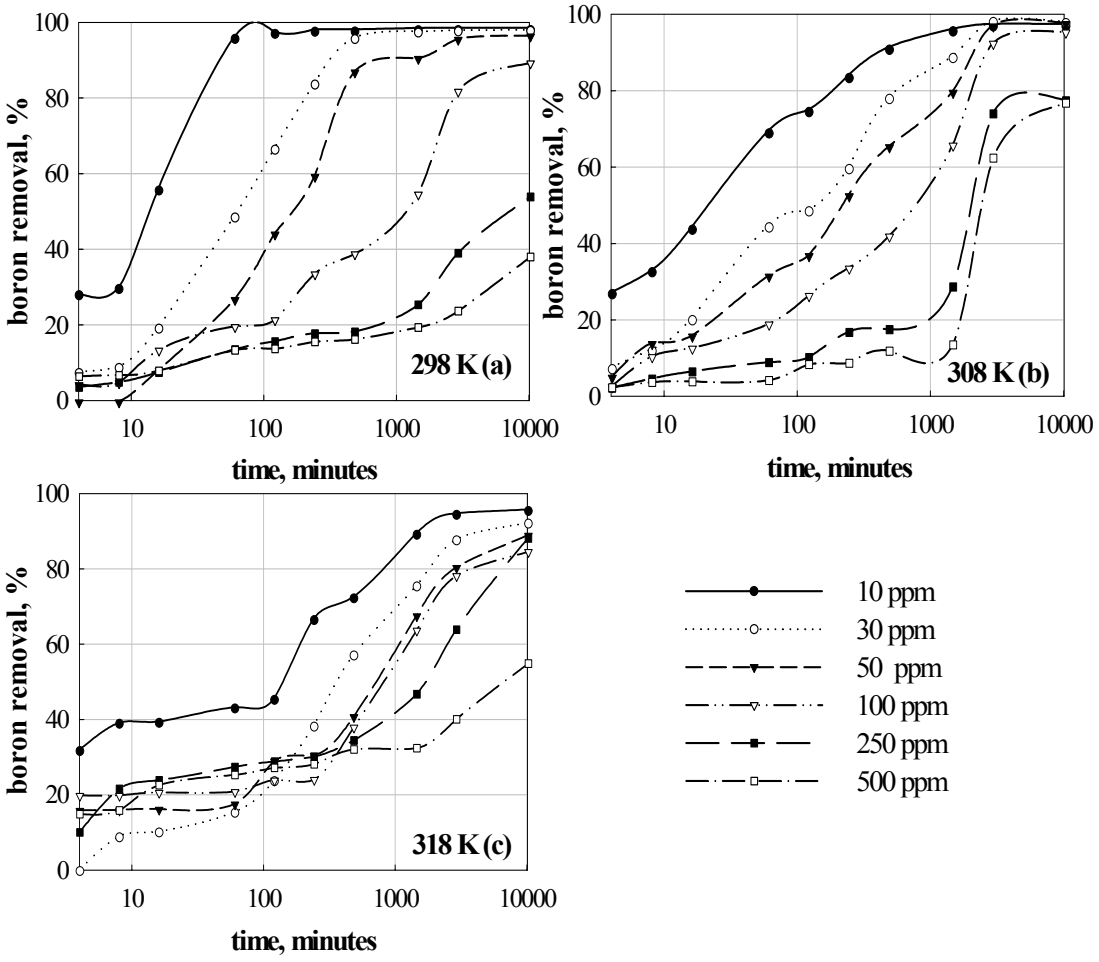

Figure 4.15. Effect of concentration on adsorption of boron for Yeniköy fly ash at 298 (a), 308 (b) and 318 K (c) (S/L=0.05, pH: natural)

The effect of temperature on the boron removal was examined at 283, 293, 303, 313, 323 and 333 K for Yeniköy ash only due to the superior adsorption capacity of this ash type over that of Soma ash. The percentage of adsorption decreased from 100 to 80 with the increase of temperature from 303 K to 333 K (the result does not change below 303 K) at a concentration of 10 mg/L and natural pH. The results obtained are presented graphically in Figure 4.16. The time period required for attainment of equilibrium was less than 8 hours at the temperatures of 283, 293, and 303 K. When temperature was furtherly increased, the equilibrium time increased beyond 48 hours. Additionally as it can be seen from tri-dimensional plots shown in Figure 4.17, the decrease in the adsorbed boron amount with increasing temperature is indicative of an exothermic nature of the sorption process. This will be further discussed in the coming section.

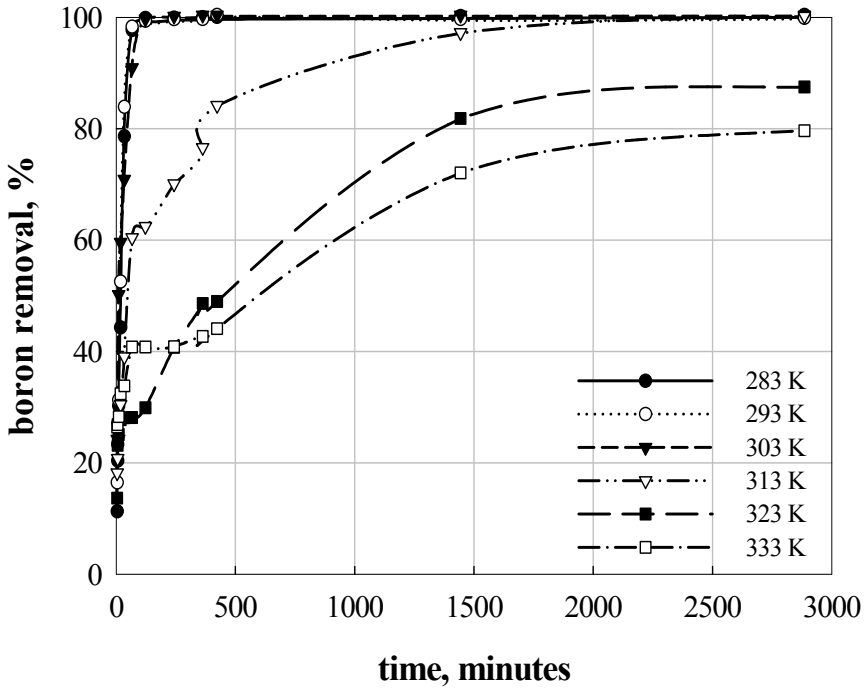

Figure 4.16. Effect of temperature on adsorption of boron for Yeniköy fly ash (initial boron concentration: 10 mg/L, S/L=0.05, pH: natural)

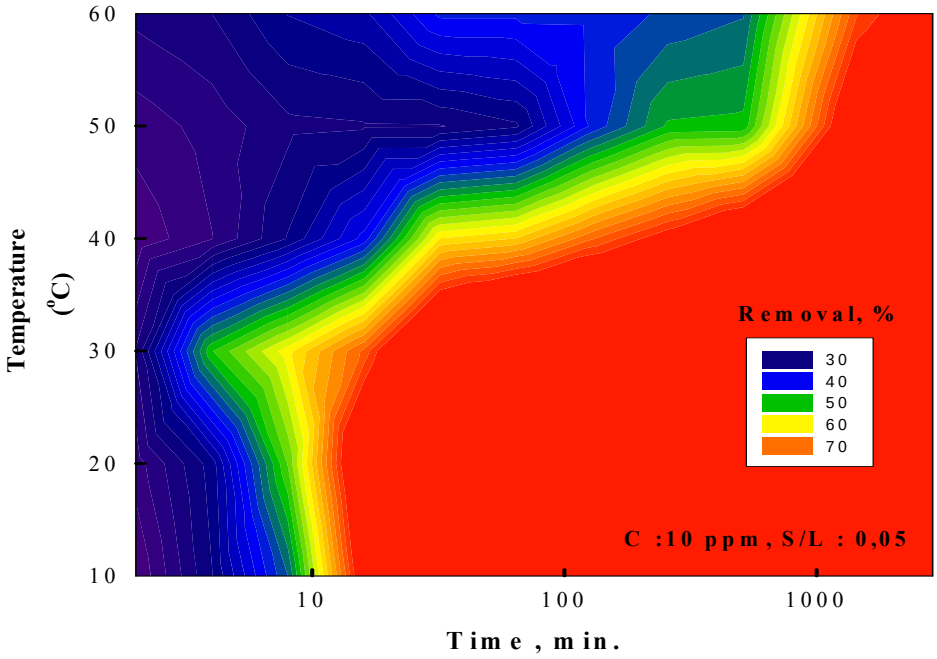

Figure 4.17. Removal of boron as a function of temperature and time for Yeniköy fly ash (initial boron concentration: 10 mg/L; pH: natural; S/L: 0.05)

4.2.4.1. Adsorption Isotherm Models

The variation of the adsorbed boron with change in liquid concentration was described using the adsorption isotherms. Adsorption isotherms are mathematical models that describe the distribution of the sorbate specie among liquid and solid phases, based on a set of assumptions that are related to the heterogeneity/homogeneity of the solid surface, the type of coverage, and the possibility of interaction between the sorbate specie.

Freundlich, Langmuir and Dubinin-Radushkevich (D-R) isotherms are commonly used to describe the adsorption characteristics utilized in water and wastewater treatment. Therefore, adsorption data of Yeniköy ash at 298, 308 and 318 K were tested using these three models.

Freundlich Isotherm

The empirically derived Freundlich isotherm is defined as follows.

$$q_e = K_f \cdot C_e^{1/n} \qquad (4.5)$$

The linearized form of Equation 4.5 can be written as follows:

$$log\ q_e = logK_f + 1/n\ log\ C_e \quad (4.6)$$

where; q_e : amount adsorbate adsorbed per unit weight of adsorbent at equilibrium

C_e : equilibrium concentration of adsorbate in solution after adsorption

K_f : empirical Freundlich constant or capacity factor (mg/g), (mol/L)

n : the Freundlich exponent (Vadivelan and Kumar 2005)

In testing the isotherm, the adsorption data is plotted as log (q_e) versus log (C_e) and should result in a straight line with slope n and intercept K_f. The intercept and the slope are indicators of adsorption capacity and adsorption intensity, respectively. The value of n falling in the range of 1-10 indicates favorable sorption (Vadivelan and Kumar, 2005).

The adsorption data which were obtained for an S/L ratio of 0.05 at neutral pH were plotted for three temperatures (298, 308 and 318 K) in the log-log form in Figure 4.18 to determine the applicability of the Freundlich isotherm to boron adsorption on Yeniköy ash. The isotherm parameters obtained by fitting the data of sorption are described by assuming that the elemental concentrations in solid and liquid are in equilibrium at the end of the experiment (48 hours).

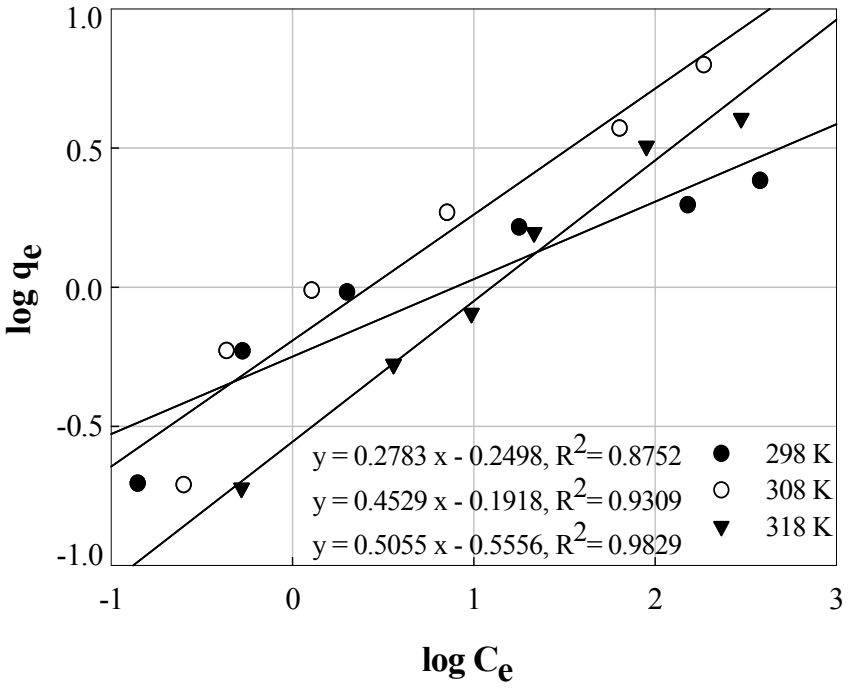

Figure 4.18. Applicability of Freundlich isotherms for Yeniköy ash (S/L=0.05, pH: Natural)

It can be seen that the data shows good linearity which is an indication of the applicability of Freundlich isotherm. This means that, adsorption steadily increases with increasing initial concentration and is not necessarily limited to monolayer adsorption. The fitting parameters in Figure 4.18 are n = 3.59, K_f = 0.56 for 298 K, n = 2.21, K_f = 0.64 for 308 K, n = 1.98, K_f = 0.28 for 318 K. The fact that *1/n* values are much below unity is suggesting a rapid decrease in the sorption capacity of the solid as the initial concentration is raised.

Langmuir Isotherm

The Langmuir adsorption isotherm is defined as

$$q_e = (q_o K_L C_e) / (1+K_L C_e) \qquad (4.7)$$

where; q_e : amount adsorbate adsorbed per unit weight of adsorbent at equilibrium

C_e : equilibrium concentration of adsorbate in solution after adsorption

q_o : empirical Langmuir constant which represents maximum adsorption capacity (mg/g)

K_L : empirical Langmuir constant (l/mg) (Vadivelan and Kumar, 2005)

Assuming the above equation (Eq. 4.7) as (Eq. 4.8)

$$C_e / q_e = (1/q_o K_L) + (1/q_o) C_e \quad (4.8)$$

and plotting of C_e / q_e vs C_e give a straight line with slope $1/q_o$ and intercept $1/q_o K_L$. In this equation, q_o, the amount adsorbed per gram of adsorbent, corresponds to complete coverage. K_L is the Langmuir constant (L/g), which is an energy constant, indicating the adsorptivity of the solute.

The data in Figure 4.18 for S/L = 0.05 at natural pH (13±0.5) for Yeniköy ash is plotted again in Figure 4.19 to test the applicability of Langmuir isotherm. As revealed by the figure, a nonlinear variation results thus suggesting that this model does not adequately describe the sorption data within the entire concentration range.

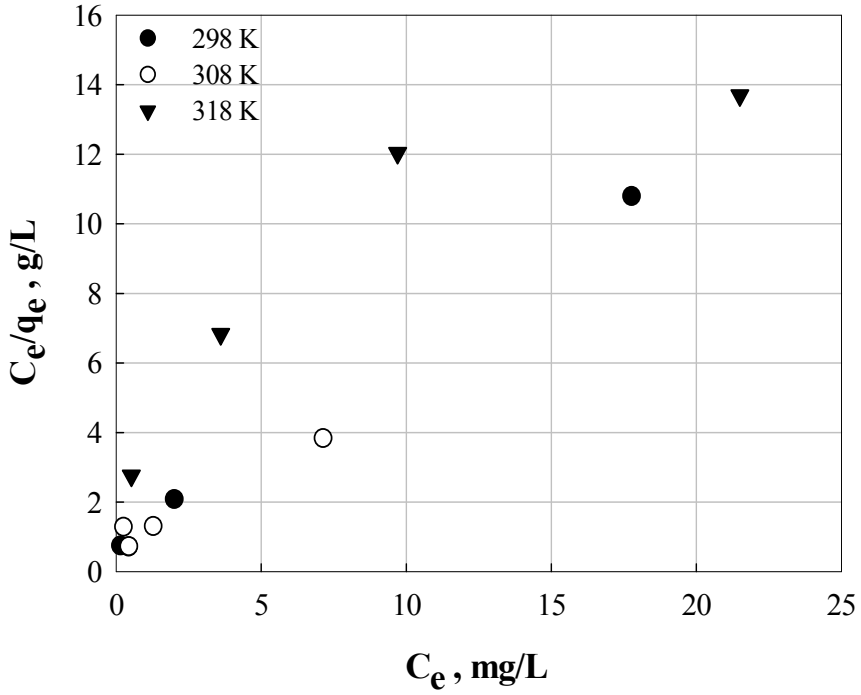

Figure 4.19. Applicability of Langmuir isotherms for boron adsorption on Yeniköy ash (S/L=0.05, pH; Natural)

D-R Isotherm

The linearized D-R isotherm model is described by the equation:

$$ln\ q_e = ln\ q_m - K\varepsilon^2 \qquad (4.9)$$

where; q_e : amount adsorbate adsorbed per unit weight of adsorbent, (mol/g)

q_m : adsorption capacity of adsorbent per unit weight, (mol/g)

K : constant related to adsorption energy, (mol^2/kJ^2)

ε : Polanyi potential, equal to $RT\ ln(1+1/C_e)$

R : gas constant, (kJ/mol·K)

T : temperature, K (Yurdakoç, et.al, 2004)

The values of q_m and K are evaluated from the intercepts and slopes of plot of ln q_e vs. ε^2. The D-R plots corresponding to sorption of boron on Yeniköy fly ash for the contact time of 48 hours and temperatures of 298, 308 and 318 K are given in Figure 4.20.

The data showed poor correlation under this model, indicating that it is not applicable under the applied sorption conditions.

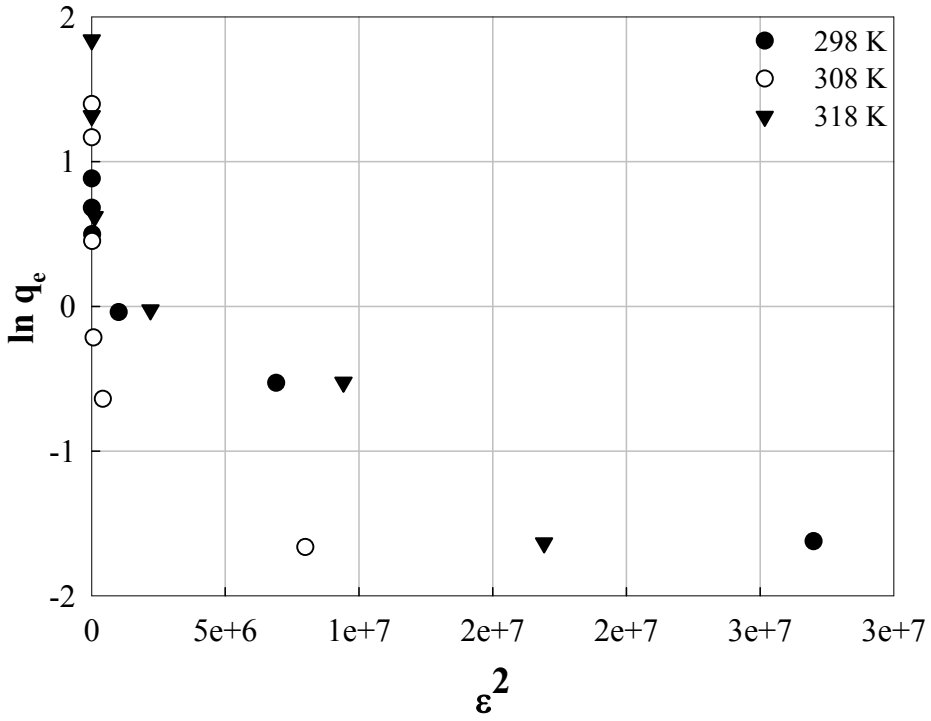

Figure 4.20. Applicability of D-R isotherms for boron adsorption on Yeniköy ash (S/L=0.05, pH; Natural)

4.2.4.2. Design of Batch Sorption from Isotherm Data

The sorption isotherm relations were applied to predict the design of single-stage batch sorption systems (Ho and Mc Kay, 1998, Vadivelan and Kumar, 2005). A schematic diagram of the mass balance of the system is shown in Figure 4.21. The design objective is to reduce the boron solution of volume V (L) from an initial concentration of C_0 to C_l (mg/L). The amount of adsorbent is M, and the solute loading changes from q_0 (mg/g) to q_1 (mg/g). At time $t = 0$, $q_0 = 0$ and as time proceeds the mass balance equates the boron removed from the liquid to that picked up by the solid.

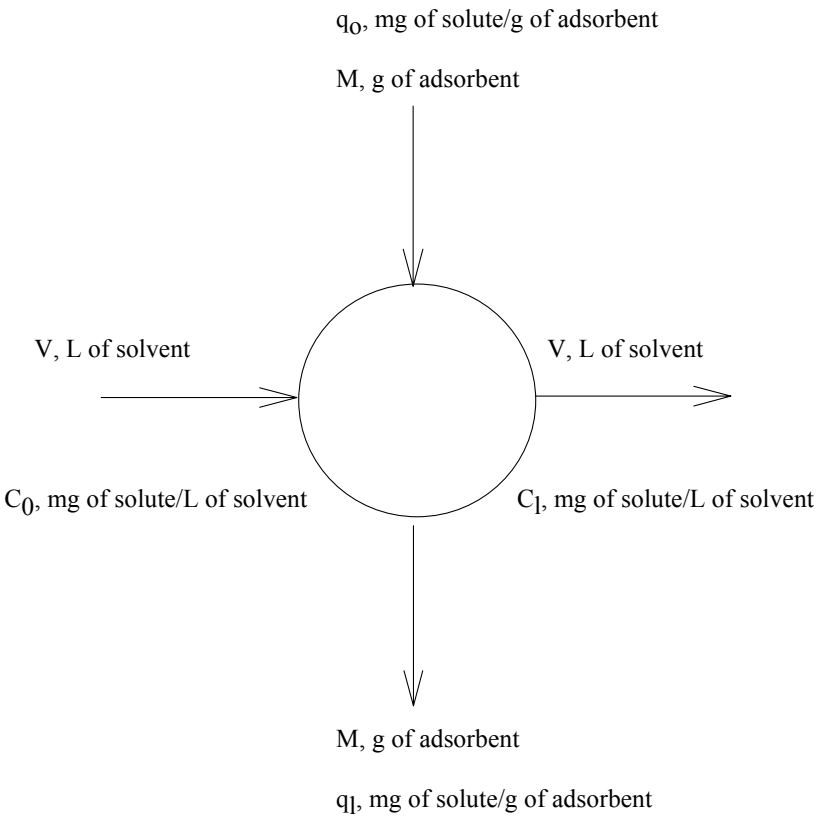

Figure 4.21. Single- stage batch adsorber design

The mass balance equation for the sorption system in Figure 4.21 can be written as

$$V(C_0 - C_l) = M(q_o - q_1) = Mq_1 \qquad (4.10)$$

Under equilibrium conditions, $C_l \rightarrow C_e$ and $q_l \rightarrow q_e$.

Since the adsorption isotherm studies confirm that the equilibrium data for boron on to Yeniköy fly ash particle fitted well in Freundlich isotherm and Freundlich isotherm equation can be used for q_l in equation batch adsorber design.

Equation 4.10 can be rearranged as

$$M/V = (C_0 - C_e)/q_e = (C_0 - C_e)/(K_f C_e^{1/n}) \qquad (4.11)$$

Figure 4.22 shows the plots of the predicted amount of ash particles required to remove a certain amount of boron from solutions of initial concentrations 100 mg/L for 60, 70, 80,and 90% boron removal at different solution volumes (1, 2, 3, 4, 5, 6, 7, 8, 9, 10 L). For a single-stage batch-sorption system, the design procedure is outlined.

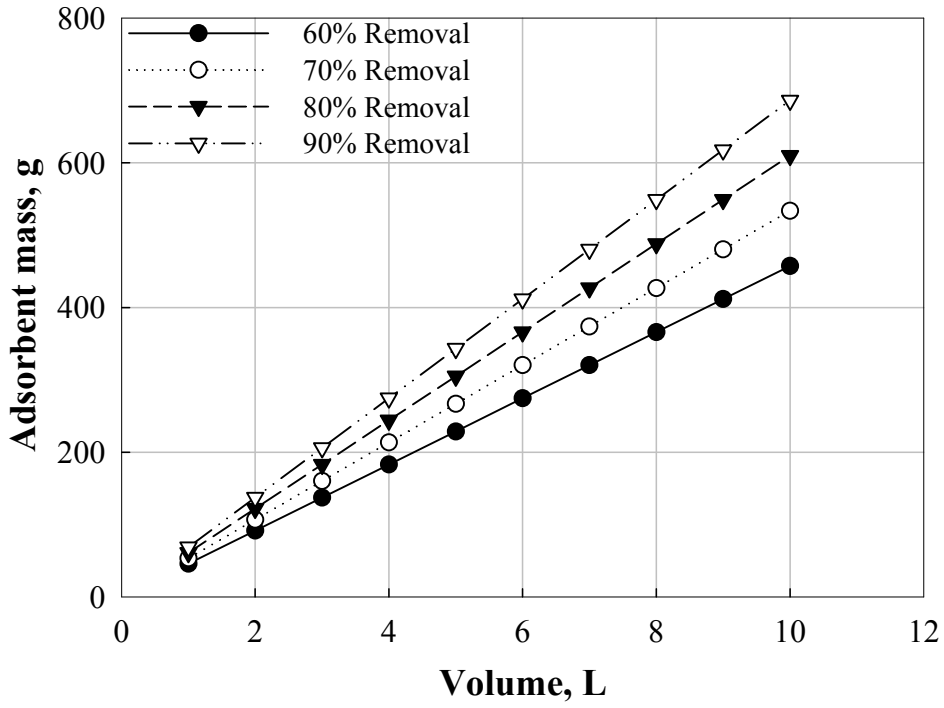

Figure 4.22. Adsorbent mass (M) against volume (L) of solution treated

4.2.4.3. Thermodynamic Parameters

The sorption data at different concentrations and temperatures were used to calculate the thermodynamic parameters ΔH° (standard enthalpy change), ΔS° (standard entropy change), and ΔG° (standard free energy). The Gibbs free energy indicates the degree of spontaneity of the sorption process and the higher negative value reflects more energetically favorable sorption. The molar free energy change of the adsorption process is related to the distribution constant (K_d) and calculated from the equation:

$$\Delta G° = -RTln\ K_d \qquad (4.12)$$

where ; R is the gas constant (8.314 J/mole K), T is the absolute temperature and the change in free energy determined. K_d values were calculated as

$$K_d = q_e / C_e \tag{4.13}$$

where q_e is the equilibrium concentration of boron on adsorbent (mg/g), C_e is the equilibrium concentration of boron in solution (mg/L).

The parameters, ΔG°, ΔS° and ΔH°, can be calculated using the following equations:

$$\Delta G^\circ = \Delta H^\circ - T\,\Delta S^\circ \tag{4.14}$$

$$\Delta H^o = R \ln \frac{K_d(T_2)}{K_d(T_1)} \left(\frac{1}{T_1} - \frac{1}{T_2}\right)^{-1} \tag{4.15}$$

The values of ΔH°, ΔS°, and ΔG° obtained for boron uptake on Yeniköy fly ash are summarized in Table 4.9. ΔH° values were calculated from the sorption data obtained at 298 and 318 K.

Table 4.8. Values of ΔH°, ΔS°, and ΔG° calculated from the sorption data

Initial Conc. (mg/L)	**ΔH°**	**ΔS°**	**ΔG° (kJ/mole)**		
	(kJ/mole)	**(J/mole·K)**	**298K**	**308K**	**318K**
10	-44,3	-88,5	-17,9	-17,1	-16,2
30	-62,3	-150,3	-17,5	-18,1	-14,5
50	-52,1	-121,5	-15,9	-17,7	-13,5
100	-17,7	-16,4	-12,8	-15,7	-12,5
250	73,6	273,4	-7,9	-9,6	-13,3
500	26,6	110,3	-6,3	-10,8	-8,5

It is seen from Table 4.9 that all the sorption cases involve negative standard Gibbs energy changes. The negative ΔG° values in fly ash indicate that the sorption of

boron is spontaneous. The extent of spontaneity decreases with increasing temperature at low concentrations and shows the opposite trend at high initial concentrations.

The standard enthalpy changes of the uptake of boron on fly ash depend on change of concentration values. Negative ΔH° values were obtained for lower initial concentrations of boron (10, 30, 50 mg/L) indicating that the processes are exothermic. On the contrary, at high concentrations, positive ΔH° values were obtained for boron sorption on fly ash indicating that the uptake process becomes endothermic.

The entropy change of the sorption process was in the range (-150)-(273). Negative entropy change is obtained at low initial concentrations, but as the concentration increases, the entropy change becomes positive. This indicates that at larger concentrations, more disorderness is associated with the sorption process. As a result of sorption reaction, negative entropy change might be expected, since such reaction causes transferring the sorbate ions from a disordered state to a more ordered state when fixed by the sorbent. However, this decrease in the disorder could be outweighed by two other factors. First one could be referred to the dehydration steps that would increase the mobility of the ions. Second one might arise from the larger number of species leaving the sorbent when a sorbate is exchanged for them, especially if the charge of that sorbate exceeds those of the ones depleted out of the sorbent matrix, e.g. two monovalent ions exchanged for one divalent ion (Akar 2005).

If ΔH° is plotted vs. ΔS° according to the equation 4-11, a linear correlation is observed (Figure 4.21). As sorption becomes endothermic, positive ΔS° values are generated. Such a correlation was reported to indicate the importance of the dehydration steps in the sorption process (Ghabbour et al. 2004).

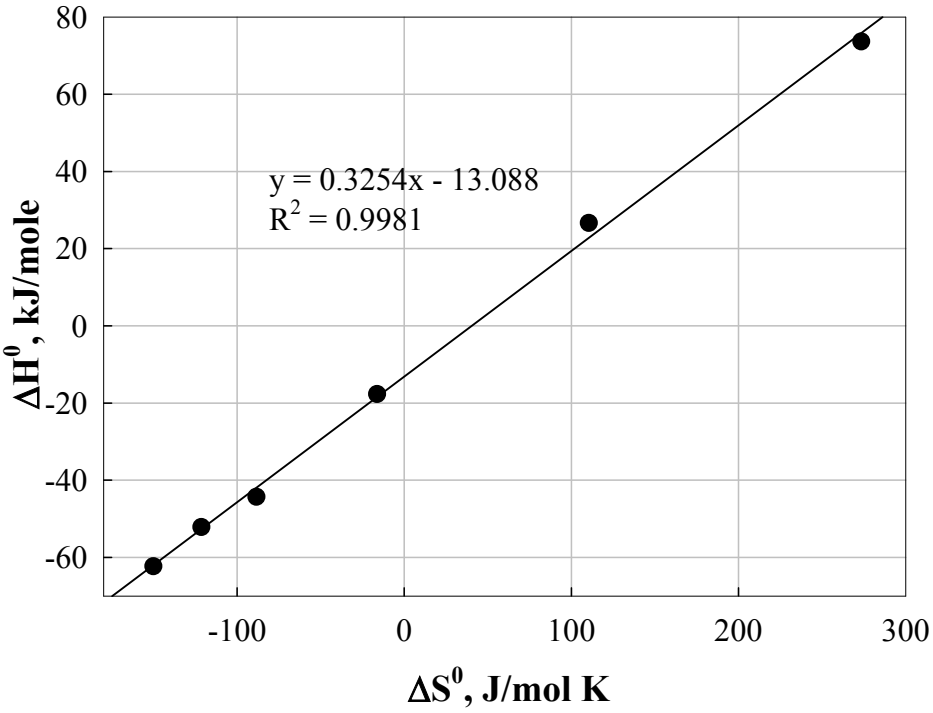

Figure 4.23. Correlation of the thermodynamic parameters in Table 4.9.

4.3. Water Quality after Boron Adsorption: Leaching of Fly Ash

The water quality with respect to heavy metals and major elements was determined using the Standard Method ASTM D-4793. The results are presented in Figure 4.22 for Yeniköy fly ash. It can be seen that most of the heavy metals do not dissolve at all and among the ones which show certain dissolution, none is above the limiting values set by the Environmental Regulations for Water Quality in Turkey for the water quality classes I, II, III and IV (Table 4.10).

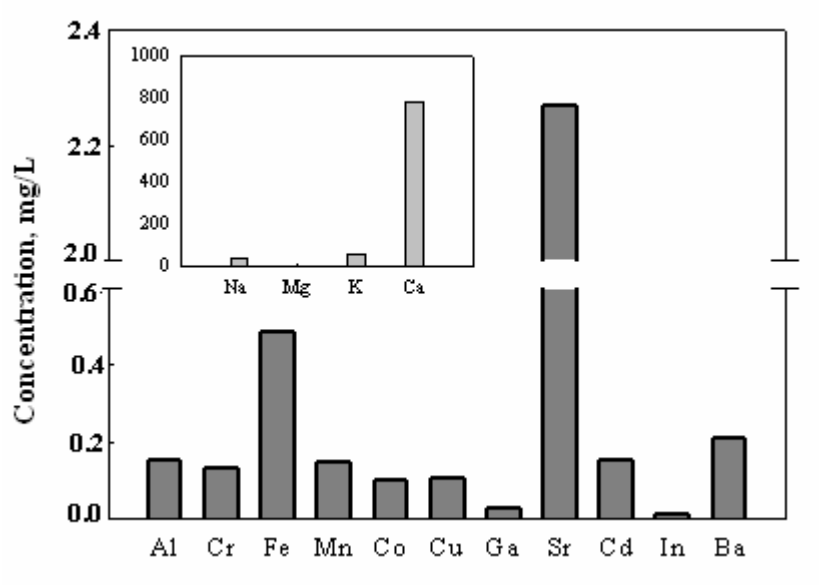

Figure 4.24. The Results of the ASTM Analysis for Yeniköy Fly Ash for Major Elements and Heavy Metals. (S/L : 1/20)

Table 4.9. Environmental Regulations for Water Quality in Turkey for the Water Quality Classes I, II, III and IV.

Inorganic Pollutants	**I. (mg/l)**	**II. (mg/l)**	**III. (mg/l)**	**IV. (mg/l)**	**Yeniköy Ash (ppb, 24h)**
Cd	3	5	10	> 10	152
Pb	10	20	50	> 50	3
Cu	20	50	200	> 200	104
Cr	20	50	200	> 200	133
Co	10	20	200	> 200	102
Ni	20	50	200	> 200	6
Zn	200	500	2000	>2000	2
Fe	300	1000	5000	>5000	486
Mn	100	500	3000	>3000	146
Ba	1000	2000	2000	>2000	209
Al	0.3	0.3	1	> 1	153

In aqueous solutions fly ash reacts with water and produces varying salinity and compositions depending on the solid / liquid ratio, extraction time and temperature. The

distribution of the metals between the soluble and the solid phases were mainly controlled by the pH of the solution and to a lesser extent by complex forming ligands such as sulfate and carbonate (Cohen et al. 2001). Desorption of these metals from the ash surfaces decreases with increasing pH but it has been also reported that, due to the high pH of the solution because of its natural buffer behavior (pH : 13± 0.5 for Yeniköy fly ash), As and some other elements are in the form of oxyanions, which are not potentially dangerous (Nathan et al. 1999). The final pH of the solutions depends on the content of the basic oxides and the amount of acidic substances such as SO_2, SO_3 and P_2O_5 which are also present in the coal fly ash. Among strong basic oxides in the combustion products, CaO undergoes to the largest variation and therefore the CaO content is the best indicator of the alkaline or neutral reaction (Corigliano et al. 1997).

CHAPTER 5

CONCLUSION

Adsorption studies were conducted to investigate the adsorption capacity of Yeniköy fly ash under different conditions such as S/L ratio, time and temperature. Based on the results of these studies the sorption was analyzed using pseudo-first-order and pseudo-second-order kinetic models. The effect of solution temperature and the determination of the thermodynamic parameters of adsorption of boron onto Yeniköy fly ash, such as activation energy, E_a , enthalpy of activation, ΔH^o , entropy of activation, ΔS^o , and free energy of activation, ΔG^o, that are important to understand the adsorption mechanism, were determined using the adsorption data. The rate and transport/kinetic processes of boron adsorption onto Yeniköy fly ash were described by applying Langmiur, Freundlich and D-R adsorption models. The specific conclusions were listed below.

1. The nominal particle size values were found to be 100 and 165 μm for Yeniköy and Soma fly ashes respectively.

2. Surface area of Yeniköy fly ash was found to be almost three times greater than the surface area of Soma fly ash and also Yeniköy ash contained larger volume of pores than Soma ash.

3. SEM images, XRD diagrams and EDX results with high standard deviations showed that the ash particles have complex structures with the surface of particles possesing a heterogeneous nature.

4. Among the materials which were tested, the ability of Yeniköy ash to remove boron was found similar to that achieved by amberlite.

5. Increasing solid/liquid ratio leads to increasing active site available for adsorption.

6. The pseudo-second-order model was more suitable for the kinetic description of the sorption process.

7. The activation energies, E_a, for the initial concentrations of 10, 30 and 50 mg/L were obtained as -99.6, -67.1 and -26.9 kJ/mole, respectively. The rate constant

decreases when temperature is increased. As the initial concentration increases, the effect of temperature, as a delaying factor for sorption, will decrease. This observation is reflected in E_a, the absolute values of which decreases with increase in initial concentration. From the values of A, it can be concluded that the fraction of boron species possessing an energy enough to overcome the activation energy barrier increases as the initial concentration is raised.

8. Negative ΔH° values were obtained for lower initial concentrations of boron (10, 30, 50 mg/L) indicating that the processes are exothermic. On the contrary, at high concentrations, positive ΔH° values were obtained for boron sorption on fly ash indicating that the uptake process becomes endothermic.

9. The entropy change of the sorption process was in the range (-150)-(273). Negative entropy change was obtained at low initial concentrations, but as the concentration increased, the entropy change became positive. This indicates that at larger concentrations, more disorderness is associated with the sorption process.

10. Negative ΔG° values were obtained indicating that the sorption of boron is spontaneous. The extent of spontaneity decreases with increasing temperature at low concentrations and shows the opposite trend at high initial concentrations.

11. Water quality following adsorption was within environmental standards as measured by the ASTM procedure. The concentration levels of major elements and heavy metals were under the standard levels defined for wastewater except for calcium.

REFERENCES

Akar, D., 2005. *Physicochemical Characterization of The Sorption Behavior of Cs^{+} and Sr^{2+} Ions on Natural Kaolinite and Clinoptilolite Minerals*, *MS. Thesis*,(İzmir).

Al-Ghouti, M., Khraisheh, M.A.M., Ahmad, M.N.M., Allen, S., 2005. "Thermodynamic Behavior and The Effect of Temperature on Removal of Dyes from Aqueous Solution Using Modified Diatomite: A Kinetic Study", *Journal of Colloid and Interface Science*, Vol. 287, pp. 6-13.

ASTM C204. 1994, *Test Method for Fineness of Portland Cement by Air Permeability Apparatus, American Society for Testing and Materials, Annual Book of ASTM Standards*, (West Conshohocken, Pennsylvania), Vol. 04.02.

Atkins, P.V, 1994. *Physical Chemistry*, (Oxford University Press, 5th Edition, Oxford).

Budavari, S. et al., 1989. *The Merck Index*, (Rahway, Merck and Co., Inc., 11th Edition).

Butterwick, L., De Oude, N., Raymond, K., 1989. "Safety Assessment of Boron in Aquatic and Terrestrial Environments", *Ecotoxicology and Environmental Safety*. Vol. 17, pp. 339-371.

Canadian Council of Ministers of the Environment, 1999. *Canadian Environmental Quality Guidelines*, (Canadian Council of Ministers of the Environment, Winnipeg).

Choi, W.W., Chen K.Y., 1979. "Evaluation of Boron Removal by Adsorption on Solids", *Environmental Science and Technology*, Vol. 13, No. 2, pp. 189-196.

Cox, J.A., Lundquist, G.L., Prazyjazny, A., Schmulbach, C.D., "Leaching of Boron from Coal Ash", *Environmental Science and Technology*, Vol. 12, pp. 722-723.

Crank, G., 1933. *The Mathematics of Diffusion*, (New York: Clarendon Press, London).

Çancı, B., 1998. *Geochemical Assessment of Environmental Effects of Fly Ash from Seyitömer Thermal Power Plant, Ms. Thesis*, (Ankara).

Data, S.P., Bahadoria, P.B.S., 1999. "Boron adsorption and desorption in some acid soils of West Bengal, India", *J. Plant Nutr. Soil Sci*., Vol. 162, pp. 183–191.

Dermatas, D., Meng, X., November 2003. "Utilization of Fly Ash for Stabilization/Solidification of Heavy Metal Contaminated Soils", *Engineering Geology*, Vol. 70, No. 3-4, pp. 377-394.

DiGioia, A. M. Jr., Nuzzo, W. L. 1977, "Fly Ash as Structural Fill", *Journal of the Power Division,* Vol. 98, No. 1, pp. 77-92.

Eisler, R., 1990. “Boron Hazards to Fish, Wildlife, and Invertebrates: A Synoptic Review”, (U.S. Fish Wildlife Service., Biological Report) Vol. 85, No.1, p. 32.

European Centre for Ecotoxicology and Toxicology of Chemicals, 1995. “Ecotoxicology of Some Inorganic Borates” Special Report, SrNo.11.

Finqueneisel, G., Zimny, T., Albiniak, A., Siemieniewska, T., Vogth, D., Weber, J.V., 1998. “Cheap Adsorbent: Active Cokes from Lignites and Improvement of Their Adsorptive Properties by Mild Oxidation”, *Fuel*, Vol. 77, pp. 549-556.

Finqueneised, G., Zimmy, T., Vogt, D., Weber, J.W., 1998. “Feasibility of the Preparation of Effective Cheap Adsorbents from Lignites in Rotary Kiln”, *Fuel Processing Technology*, Vol. 57, p. 196.

Ghabbour, E.A., Davies, G., Goodwillie, M.E., O’Donaughy, K., Smith, T.L., 2004. “Thermodynamics of Peat-, Plant-, and Soil-derived Humic Acid Sorption on Kaolinite”, *Environmental Science and Technology*, Vol. 38, pp. 3338-3342.

Goldberg, S., Forster, H.S., Lesch, S.M., Heick, E.L., 1996.“Influence of anion competition on boron adsorption by clay minerals and soils”, *Soil Sci*., Vol. 161, No. 2, pp. 99–103.

Grinstead R.R, Wheaton R.M., 1971. “Improved Resins for the Removal of Boron from Saline Water-exploratory Study”, (Research and Development Progress Report) No. 721.

Gupta, U.C., James Y.W., Campbell C.A., Leyshon, A.J., Nicholaichuk W., 1985. “Boron Toxicity and Deficiency: A Review”, *Canadian Journal of Soil Sciences*, Vol. 65, pp. 381-409.

Hayashi H., Iwasaki T., Onodera Y. and Torii K., 1991. “Boron Adsorption on Hydrous Cerium Oxide in Hydrothermal Conditions”, In New Developments in Ion Exchange, Proceedings of the International Conference on Ion Exchange, ICIE’91, Tokyo, Japan, (2 - 4 October 1991), eds M. Abe, T. Kataoka and T. Suzuki, Elsevier, pp. 553-558.

Health Canada, 1990. *Guidelines for Canadian Drinking Water Quality*, (Supporting Documentation, Part III, Boron, Edited on May 1991).

Ho, Y.S., McKay, G., 1998. “The Kinetics of Sorption of Divalent Metal Ions Onto Sphagnum Moss Peat”, *Can. J. Chem. Eng*., Vol. 76, pp. 736-739.

Ho, Y.S., McKay, G., 2000. “The Kinetics of Sorption of Divalent Metal Ions Onto Sphagnum Moss Peat”, *Water Research*, Vol. 34, pp. 736-739.

James, W.D., Graham, C.C., Glascock M.D., Hanna, A.S.G., 1982. “Water-leachable Boron from Coal Ashes”, *Environmental Science and Technology*, Vol. 16, pp. 195-197.

Kabay, N., Yılmaz, I., Yamaç, S., Samatya, S., Yüksel, M., Yüksel, U., Arda, M., Sağlam, M., Iwanaga, T., Hirowatari, K., 2004. "Removal and Recovery of Boron from Geothermal Wastewater by Selective Ion Exchange Resins. I. Laboratory Tests", *React. Funct. Polym.,* Vol. 61, No. 3.

Kaftan, Ö., 2004. *A Novel Sorbent (MCM-41 Immobilized with N-Methylglucamine) for Removal/Preconcentration of Boron from Waters. Synthesis, Characterization and Applications to Water Samples*, *Ms. Thesis*, (İzmir).

Kannan N., Sundaram M.M., 2001, "Kinetics and Mechanism of Removal of Methylene Blue by Adsorption on Various Carbons - A Comparative Study", *Dyes and Pigments*, Vol.51, pp. 25-40.

Keren, R., Groosl, P.R., Sparks, D.L., 1994. "Equilibrium and Kinetics of Borate Adsorption-Desorption on Pyrophyllite in Aqueous Suspensions", *Soil Sci. Soc. Am. J*., Vol.58, pp. 1116–1122.

Kılıç, A.M. 2004. "Importance of Boron Mine for Turkey and Place in the Future", Proceedings of the 2nd International Boron Symposium, Eskişehir, (23-25 September 2004), p. 34.

Kunin R., Preuss A.F., 1964. "Characterization of A Boron-specific Ion Exchange Resin", *Industrial and Engineering Chemistry: Product, Research and Development*, Vol:3, No:4, pp. 304-306.

Lapp, T.W., Cooper, G.R., 1976. "Chemical Technology and Economics in Environmental Perspectives in Removal of Boron from Wastewater", (EPA Office of Toxic Substances Institute Kansas City).

Levine, I.N., 1988. *Reaction Kinetics and Surface Chemistry in Physical Chemistry*, (McGraw Hill, 3rd Edition, Singapore), p. 372, 373, 537-540.

Liu, D., Hsu, C., Chuang, C., 1995, "Ion-exchange and Sorption Kinetics of Cesium and Strontium in Soils", *Appl. Radiat. Isot*., Vol:46, pp. 839-843.

Lyman, W.R., Preuss A.F., 1957. "Boron Adsorbing Resin and Process for Removing Boron Compounds From Liquids", (U.S. Patent No. 2813838 (Rohm & Haas Company)).

Ma, B., Qi, M., Peng, J., Li, Z., 1999. "The Compositions, Surface Texture, Absorption, and Binding Properties of Fly Ash in China", *Environment International*. Vol:25, No:4, pp. 423-432.

Magara, Y., Aizawa, T., Kunikane, S., Itoh, M., Kohki, M., Kawasaki, M., Taeut, H., 1996. "The Behavior of Inorganic Constituents and Disinfection by Products in Reverse Osmosis Water Desalination Process", *Water Science Technology*, Vol:34, pp. 141-148.

Magara, Y., Tabata, A., Kohki, M., Kawasaki, M., Hirose, M., 1998. ”Development of Boron Reduction System for Sea Water Desalination”, *Desalination*, Vol:118, pp. 25-34.

Matsumoto, M., Kondo, K., Hirata, M.S., Kokubu, T., Hano, Takada, T., 1977. ”Recovery of Boric Acid from Wastewater by Solvent Extraction”, *Separ. Sci. Technol*., Vol. 32, No. 5, pp. 983-991.

Matsumoto, M., Matsui, T., Kondo, K.J., 1999. “Adsorption Mechanism of Boric Acid on Chitosan Resin Modified by Saccharides“, *Chem. Eng. Jpn*., Vol. 32, No. 2, pp. 190–196.

McKerall, W.C., W.B. Ledbetter, and D. J. Teague, 1982. Analysis of Fly Ashes Produced in Texas. (Texas Transportation Institute, Research Report No. 240-1, Texas A&M University, College Station, Texas).

Melnik, L., Vysotskaja, O., Kornilovich, B., 1999. “Boron Behavior During Desalination of Sea and Underground Water by Electrodialysis“, *Desalination*, Vol:124, pp. 125-130.

Metcalf, Eddy, 2003. *Wastewater Engineering: Treatment and Reuse*, (McGraw Hill International Edition, New York).

Meyers, J.F., Pichumani, R., Kapples, S.B., 1976. Fly Ash: A Highway Construction Material, (Federal Highway Administration, Report No. FHWA-IP-76-16, Washington, DC).

Montgomery J.M., 1985. *Water Treatment Principles and Design*, (Consulting Engineers Inc. USA).

National Academy of Sciences (NAS), 1980. “Boron; Mineral Tolerance of Domestic Animals”, Natl. Acad. Sci., Natl. Res. Counc., Comm. Anim. Nutr. Washington, D.C, pp. 71-83.

Nicholaichuk, W., Leyshon, A.J., Jame, Y.W., Campbell, C.A., 1988. “Boron and Salinity Survey of Irrigation Projects and the Boron Adsorption Characteristics of Some Saskatchewan Soils”, *Can. J. of Soil Science*, Vol:68, No:1, pp. 77-90.

Okay O., Güçlü H., Soner E., Balkaş, T., 1985. “Boron Pollution in the Simav River, Turkey and Various Methods of Boron Removal”, *Water Res*., Vol:19, No:7, pp.857-862.

Ooi, K., Katoh, H., Sonoda, A., Hirotsu, T., 1996. “Screening of Adsorbents for Boron in Brine”, *Ion exchange*,Vol:7, No:3.

Özcan, A.S., Özcan, A., 2004. “Adsorption of Acid Dyes from Aqueous Solutions onto Acid-activated Bentonite”, *Journal of Colloid and Interface Science*, Vol.276, Issue.1,pp.39-46

Peak, D., Luther, G.W., Sparks, L., 2003. "ATR-FTIR spectroscopic studies of boric acid adsorption on hydrous ferric oxide", *Geochim. Cosmochim. Acta*, Vol:67, No:14, pp. 2551-2560.

Peterson, W.D., 1975. Removal of Boron from Water, (Us patent 3,856,670; CA, 83, 102888b).

Pilipenko, A.T., Grebenyurk, V. D., Melnick, L.A., 1990. "Extraction of Boron Compounds from Natural Waste Water and Industrial Effluents", *Khimiya I Tekhnologuiya Vody*, Vol:12, No:3, pp. 195-210.

Polat, H., Vengosh, A., Pankratov, I., Polat, M., 2003. "A New Methodology for Removal of Boron from Water by Coal and Fly Ash", *Desalination*. Vol.164, No.2, pp.173-188

Popat, K.M., Anand, P.S., Dasare, B.D., 1988. "Synthesis and Characterization of Boron Selective Porous Condensate Cation Exchanger", *Reactive Polymers*, Vol:8, pp. 143-151.

Puls, R., 1994. *Mineral Levels in Animal Health: Diagnostic Data*, (Sherpa International, Clearbrook, British Columbia, 2nd Edition).

Recepoğlu O., Beker Ü., 1991. "A Preliminary Study of Boron Removal from Kizildere/Turkey Geothermal Waste Water", *Geothermics N.*, Vol:20 No:1-2, pp. 83-89.

Rio, S., Delebarre, A., January 2003. "Removal of Mercury in Aqueous Solution by Fluidized Bed Plant Fly Ash", *Fuel*, Vol:82, Issue:2, pp. 153-159.

Ristic M. Dj., Rajakovik Lj. V., 1996. "Boron Removal by Anion Exchangers Impregnated with Citric and Tartaric Acids", *Separation Science and Technology*, Vol:31 No:20, pp. 2805-2814.

Rouquerol, F., 1999. *Adsorption by Powders and Porous Solids*, (Academic Press, London), pp. 1-21, 355-361, 378-382.

Sawyer, N.C., Mc Carty, P.L., Parkin, G.F., 1994, *Chemistry for Environmental Engineering*, (Mc. Graw Hill International Edition, Singapore).

Schilde, U., Uhlemann, E., 1992. "A Simple Method for the Control of Ion-exchange Process with Boric Acid Using Specific Chelating Resins", *React. Polym.*, Vol:18, pp. 155-158.

Schwarzenbach, R.P, Gschwend, M.P, Imboden, D.M., 2003. *Environmental Organic Chemistry*, (John Wiley & Sons, Inc. Publication, Canada).

Seal, B.S., Weeth, H.J., 1980. "Effect of Boron in Drinking Water on the Male Laboratory rat, Bull", *Environ. Contam. Toxicol.*, Vol:25, pp. 782-789.

Shahwan, T., Erten, H.N. 2002. "Thermodynamic Parameters of Cs^+ Sorption on natural Clays", *Journal of Radioanalytical and Nuclear Chemistry.* Vol. 253, pp. 115-119.

Simonnot, M.O., Castel, C., Nicolaie, M., Rosin, C., Sardin, M., Jauffret, H., 2000. "Boron Removal from Drinking Water with A Selective Resin", *Water Research*, Vol:34, No:1, pp.109-116.

Singh, K.K., Rastogi, R., Hasan, S.H., 2005. "Removal of Cr(VI) from Wastewater Using Rice Bran", *J. Hazard. Material*, Vol:123, No:1-3, pp. 51-58.

Smith, B. M., Todd, P., Bowman, C. N., 1995. "Boron Removal by Polymer, Assisted Ultrafiltration", *Separ. Sci. Technol*., Vol:30, No:20, pp. 3849-3859.

Song D., Huang L., 1987. "The Design of A 200 m3/d Deboronation System and Its Field Trials on Xisha Islands", *Water Treatment*, Vol:2, pp. 141-147.

Su, C., Suarez, D., 1995. "Coordination of adsorbed boron: A FTIR spectroscopic study" *Environ. Sci. Technol*., Vol:29, pp. 302–311

Şahin, S., 1996. "Mathematical Model of Boron Adsorption by Ion Exchange", *ACH: Models Chem*., Vol:133, No:1-2, pp. 143-150.

Vadivelan, V., Kumar, K.V., 2005. "Equilibrium, Kinetics, Mechanism, and Process Design for the Sorption of Methylene Blue onto Rice Husk", *Journal of Colloid and Interface Science*, Vol. 286, pp. 90-100.

Yurdakoç, M., Seki, Y., Karahan, S., Yurdakoç, K., 2005. "Kinetic and Thermodynamic Studies of Boron Removal by Siral 5, Siral 40 and Siral 80", *Journal of Colloid and Interface Science*, Vol. 286, Issue 2, pp. 440-446.

Walker, C.T., 1975. *Geochemistry of Boron* (Dowden, Hutchinson&Ross, New York), pp. 47-63

WEB_1, 2005. Türkiye Toprak İlmi Derneği, Bildiri Özetleri, 15.03.2005. http://www.toprak.org.tr/isd/isd_17.htm

WEB_2, 1996. Environmental Protection Agency (EPA), 29.08.2003. http://www.epa.gov/OST/Tools/dwstds.html

Weshe, K., 1991, Fly Ash in Concrete Properties and Performance Report of Technical Committee 67-FAB, (Use of Fly Ash in Building Ritem Report 7, London, New York), pp. 5-22, 160-177.

World Health Organization, 1998, Guidelines for Drinking-water Quality, 2nd ed. Addendum to Vol. 2. Health criteria and other supporting information. Geneva, pp. 15-29.